Medizinische Fakultät

der

Universität Duisburg-Essen

Aus der Klinik für Innere Medizin

Evaluation of a liquid biopsy approach in pancreatic ductal adenocarcinoma

I n a u g u r a l d i s s e r t a t i o n

zur

Erlangung des Doktorgrades der Medizin

durch die Medizinische Fakultät

der Universität Duisburg-Essen

Vorgelegt von

Isabel Marie Rudolph

aus Essen

2022

DOI: 10.17185/duepublico/78168
URN: urn:nbn:de:hbz:465-20230413-095555-6

Dekan:	Herr Univ.-Prof. Dr. med. J. Buer
1. Gutachter:	Herr Univ.-Prof. Dr. med. J. Siveke
2. Gutachter:	Herr Univ.-Prof. Dr. med. A. Rösch

Tag der mündlichen Prüfung: 20. Januar 2023

TABLE OF CONTENTS

1 INTRODUCTION

1.1 Pancreatic cancer

1.1.1 Epidemiology

Despite years of laboratory and clinical research, pancreatic cancer remains a severe disease with a poor prognosis. In 2016, 18.400 people in Germany were diagnosed with pancreatic cancer and almost the same amount of patients died from this diagnosis, making it the fourth leading cause of cancer related deaths in Germany (RKI, 2016). The incidence has been rising continuously over the last years, and recent investigations assume that pancreatic cancer will rank as the second most common cause of cancer related deaths in Germany by 2030 (Quante et al., 2016). Demographic aging of the population and increasing occurrence of risk factors such as obesity and diabetes are known to enhance this development (Ma et al., 2013).

1.1.2 Histology

Malignant neoplasms of the exocrine pancreas can be divided into neoplasms originated from ductal cells and from acinar cells. With an amount of more than 90% the pancreatic ductal adenocarcinoma (PDAC) originated from ductal cells is the most frequent subtype of pancreatic cancer (Cascinu et al., 2010). Additionally, PDAC can be divided into seven histologic subcategories according to its microscopic appearance (Bosman et al., 2010).

1.1.3 Pathogenesis and mutational landscape

The most frequently found oncogenic driver mutations in pancreatic cancer are activating mutations in the Kirsten Rat Sarcoma (*KRAS*) gene, which occur in more than 90% of pancreatic cancers (Bailey et al., 2016; Forbes et al., 2011). *KRAS* is a protooncogene and regulates cell proliferation, differentiation, apoptosis and cell migration through interaction with signaling

molecules. Thus, a *KRAS* activating mutation can induce malignant differentiation in cells and stimulate tumor growth (di Magliano & Logsdon, 2013). A mutation of *KRAS* is detectable in more than 90% of premalignant lesions in PDAC, and the frequency of mutant *KRAS* cells increases with the degree of dysplasia, suggesting that this mutation is a critical initiating event in the carcinogenesis of pancreatic cancer (Kanda et al., 2012). Studies on mouse models have reported that growth and maintenance of pancreatic cancer as well as its metastatic lesions depend on the continuity of the oncogenic *KRAS* signaling (Collins et al., 2012a; Collins et al., 2012b). Missense substitutions account for the majority of *KRAS* mutations in pancreatic cancer. In specific, the most frequent mutational event observed in the *KRAS* gene is a point mutation on codon 12 of exon two, which leads to a replacement of the GGT sequence (Bournet et al., 2016). According to the Catalogue of Somatic Mutations in Cancer (COSMIC), approximately half of mutant *KRAS* genes contain a GAT sequence instead of the GGT sequence, forming the G12D mutation. Less frequent mutations are, named in decreasing incidence, the G12V, G12R, G12C, G12S and G12A mutations (Forbes et al., 2011). Occasionally, point mutations also occur on codon 13 and 61, resulting in the G13D, Q61L or Q61H mutation (Forbes et al., 2011). These mutational loci are common targets in *KRAS* screening kits, as their combined detection theoretically allows to identify more than 90% of *KRAS* mutations. In spite of recent successes in targeting *KRAS* G12C mutations, which are rare in PDAC, no drug has been clinically developed yet that effectively targets *KRAS* mutations (Janes et al., 2018).

Further high-frequent driver mutations in pancreatic cancer interact with the G1/2 checkpoint in the cell cycle. Among these are inactivating events in the tumor suppressor genes tumor protein 53 (*TP53*) and cyclin dependent kinase inhibitor 2A (*CDKN2A*), which occur between 50% and up to 80% of patients, respectively (Bailey et al., 2016; Waddell et al., 2015).

The transforming growth factor beta pathway (TGF-beta) is a molecular pathway involved in epithelial-mesenchymal transition and stromal biology, both hallmarks of PDAC, that is frequently affected by mutational events. Most of them occur in the tumor suppressor gene decapentaplegic homolog 4 (*SMAD4*), which is mutated in about half of PDAC patients (Bailey et al., 2016).

1.1.4 Characteristics of pancreatic cancer

Multiple reasons for the devastating prognosis of this cancer entity have been described. One of them is the interindividual as well as intraindividual mutational heterogeneity beyond the alterations in the four aforementioned genes. Studies have described an average of 63 mutated genes in each cancer, complicating the development of effective targeted therapies (Jones et al., 2008).

Further, 80% of patients are diagnosed in the late clinical stage of locally advanced or metastatic disease, when curative treatment is not feasible. The late diagnosis is largely attributable to the lack of specific symptoms in early stages and efficient screening methods (Vincent et al., 2011).

Moreover, pancreatic cancer typically induces a dense collagenous stroma within the tumor microenvironment, which is referred to as desmoplastic reaction. Due to the fibrotic characteristics of this stroma, therapeutic drugs may have difficulty accessing cancer cells, resulting in an impaired response (Provenzano et al., 2012). Among other cells, pancreatic stellate cells show increased proliferation in cancer derived desmoplastic stroma and contribute to an immunosuppressive microenvironment, contributing to cancer development and immune evasion (Apte et al., 2004; Ene-Obong et al., 2013). Further investigations showed that pancreatic stellate cells can alter the cancer metabolism by secreting non-essential amino acids, which reduces the cancer's dependency on glucose- and glutamine-derived carbon to fuel the tricarboxylic acid cycle (Sousa et al., 2016). The combination of these and likely additional other factors distinguishes pancreatic cancer from other less aggressive malignancies and contributes to the unchanged impaired prognosis over the years.

1.1.5 Clinical appearance

The symptoms associated with this malignancy depend, amongst other factors, on the location of the tumor. The majority of pancreatic tumors are located in the head, while only 20% are found in the body or tail of the organ (Ducreux et al., 2015). Clinical presentation mostly starts in the state of infiltration of surrounding tissue or metastatic spread to distant organs. Usually, first symptoms

of patients are unspecific and include abdominal pain, mid back pain, weight loss and impaired glucose tolerance. These symptoms often occur months before the diagnoses and are then attributed to the disease, retrospectively. More specific symptoms are obstructive jaundice, venous thrombosis and gastric-outlet obstruction causing nausea and vomiting or even pancreatitis (Cascinu et al., 2010; Vincent et al., 2011; Zhang et al., 2018).

1.1.6 Diagnostics

Imaging modalities in the diagnostic workup of PDAC mainly rely on computed tomography (CT), magnetic resonance imaging (MRI) and endoscopic ultrasound (EUS) along with tissue examination (Cascinu et al., 2010). The CT is the most frequently used imaging modality, best performed as multi-detector CT (Al-Hawary et al., 2014). The multi-detector CT reaches a sensitivity and specificity of 89% and 90% for the detection of pancreatic cancer. The MRI reaches a similar sensitivity and specificity but is less frequently used due to its high costs and few availability (Treadwell et al., 2016; Zhang et al., 2018). EUS has higher sensitivity and specificity rates than the above mentioned techniques, especially when combined with fine needle aspiration and cytological diagnostics (Agarwal et al., 2004). Due to its invasive character, EUS is mostly performed after noninvasive imaging modalities have been carried out (Zhang et al., 2018).

Biomarker analysis complements imaging modalities in the diagnosis and treatment of symptomatic patients. The best described blood-based biomarker for pancreatic cancer is carbohydrate antigen 19-9 (CA 19-9). Studies reported that an increased CA 19-9 level prior to surgery or chemotherapy can predict early relapse and correlates with poor survival (Bernard et al., 2019; Toledano-Fonseca et al., 2020). Screening asymptomatic patients for early-stage pancreatic cancer however exceeds the ability of this biomarker (Kim et al., 2004). This can be explained by the fact that CA 19-9 is also increased in other malignancies and in benign conditions such as biliary infection, inflammation or obstruction (Marrelli et al., 2009; Poruk et al., 2013; Zhang et al., 2018). Furthermore, 6% of Caucasian people and 22% of the African American population are Lewis antigen negative, so they do not produce CA 19-9 (Tempero et al., 1987). Even though the prognostic value of CA 19-9 has been proven in many studies, these characteristics limit the

reliability of this biomarker and explain why more potent alternatives in the management of pancreatic cancer are needed (Zhang et al., 2018).

1.1.7 Classification and staging

Pancreatic cancer stages are classified regarding to the 8th edition of TNM criteria (Cong et al., 2018). Tumor size is indicated by the T stage. N and M stage refer to the presence of tumor metastasis in lymphatic nodes or other distant sites. Prognostic staging is performed according to the American joint Committee on Cancer/ Union for international Cancer Control (AJCC/UICC), which is based on the TNM classification (Al-Hawary et al., 2014).

Table 1. 8th edition of TNM criteria and AJCC/UICC staging of pancreatic cancer (Cong et al., 2018).

Primary Tumor (T)	
pTX	Primary tumor cannot be assessed
pTis	Carcinoma in situ
pT1	Tumor ≤ 2 cm in greatest dimension
pT1a	Tumor ≤ 0.5 cm in greatest dimension
pT1b	Tumor > 0.5 and < 1 cm in greatest dimension
pT1c	Tumor 1 – 2 cm in greatest dimension
pT2	Tumor > 2 cm and ≤ 4 cm in greatest dimension
pT3	Tumor > 4 cm in greatest dimension
pT4	Tumor involves celiac axis, superior mesenteric artery or common hepatic artery, regardless of size

Lymphatic node (N)	
pNX	Regional lymph nodes cannot be assessed
pN0	No regional lymph node involvement
pN1	Metastasis in one to three regional lymph nodes
pN2	Metastasis in four or more regional lymph nodes

Distant metastasis (M)	
pM0	No distant metastasis
pM1	Distant Metastasis

Staging Groups			
Stage 1A	T1	N0	M0
Stage 1B	T2	N0	M0
Stage 2A	T3	N0	M0
Stage 2B	T1-3	N1	M0
Stage 3	T1-3	N2	M0
	T4	Any N	M0
Stage 4	Any T	Any N	M1

1.2 Treatment of pancreatic cancer

Treatment options in pancreatic cancer depend on the initial assessment as curative or palliative disease. Pancreatic cancer can only be cured by complete surgical resection of the tumor, which is possible in UICC stage I and II as well as stage III patients categorized as borderline resectable. For inoperable patients with stage III locally advanced disease and in patients with stage IV metastatic disease, palliative treatment is an option (Wolfgang et al., 2013).

1.2.1 Curative setting

Neoadjuvant chemotherapy, surgical resection and adjuvant chemotherapy are the most important treatment options in the curative setting. Neoadjuvant chemotherapy is still controversially discussed given the lack of randomized controlled trials. In borderline resectable patients, neoadjuvant chemotherapy was able to increase the total resection rate and the rate of resections without residual tumor (R0) and states a notable option for these patients. The choice of the most effective chemotherapeutic regimen in the neoadjuvant setting is subject of recent studies (Kunzmann et al., 2021).

For operable patients, primary resection and adjuvant chemotherapy remain the standard of care (Wolfgang et al., 2013; Zhan et al., 2017).

A pancreaticoduodenectomy is performed when the tumor is located in the head of the pancreas, or a distal pancreatectomy with en-bloc splenectomy when it is located in the body or tail (Lambert et al., 2019). These operations inherit a high risk of morbidity ranging from 20-75% of patients and a mortality of around 1-10% (Birkmeyer et al., 2002; Cameron et al., 2006; Wolfgang et al., 2013).

Following surgical resection, an adjuvant chemotherapy is recommended. The modified FOLFIRINOX regimen, consisting of oxaliplatin, irinotecan, leucovorin and fluorouracil, is the preferred adjuvant treatment for patients with a good performance status. Gemcitabine as monotherapy or in combination with capecitabine is an option for frail patients or those with contraindications for FOLFIRINOX (Conroy et al., 2018; Lambert et al., 2019).

1.2.2 Palliative setting

The best approach in the palliative setting depends on the patient's performance status. Patients with good performance status are eligible for systemic therapy, whereas patients with poor performance status are recommended to receive best supportive care (Wolfgang et al., 2013). The PRODIGE4/ACCORD 11 study was the first randomized phase 2/3 study to demonstrate the superiority of FOLFIRINOX as combination therapy towards gemcitabine monotherapy in the palliative setting. With an overall survival of 11.1 months, compared with 6.8 months and a progression-free survival of 6.4 months, compared with 3.3 months, a benefit of the FOLFIRINOX regimen was evident (Conroy et al., 2011). Another therapy that showed superiority in metastatic patients over gemcitabine monotherapy is gemcitabine combined with nab-paclitaxel. An overall survival of 8.5 months was achieved with this combination therapy compared with 6.7 months with gemcitabine alone (Von Hoff et al., 2013). Current state of research declares both combination therapies as suitable for the treatment of metastatic disease, few trials however allowed a direct comparison of the two treatment regimens in 1st line treatment. Retrospective meta-analysis on this topic suggests that the difference in terms of survival and progression are marginally and the decision in favor of one treatment should depend on the individual age, performance status, toxicity and previous therapies (S. Kim et al., 2018; Pusceddu et al., 2019).

Furthermore, the NAPOLI-1 trial reported a benefit for the combination of nanoliposomal irinotecan, 5-fluoruracil (5-FU) and folinic acid in the 2nd line treatment, when gemcitabine-based regimens were given in 1st line treatment. Patients receiving the combination therapy with nanoliposomal irinotecan had a longer overall survival with a median of 6,1 months, compared with a median overall survival of 4.2 months in patients receiving 5-FU and folinic acid alone. Progression-free survival and objective response rate were also increased in patients receiving the nanoliposomal irinotecan combined therapy (Wang-Gillam et al., 2016). According to this study, the guidelines recommend the combination of 5-FU, folinic acid and nanoliposomal irinotecan for patients with good performance status after failure of a 1st line gemcitabine-based treatment (Oettle & Lehmann, 2016). Fit patients who received FOLFIRINOX as 1st line treatment may receive

gemcitabine with our without nab-paclitaxel combination as 2nd line treatment (Lambert et al., 2019).

1.2.3 Value of mutational detection for precision medicine in pancreatic cancer

At this point of clinical standard, detection of the common driver mutations does not represent a decisive element in the selection of systemic treatment (Aguirre et al., 2018). However, the detection of less frequent mutations may result in specific treatment recommendations.

Approximately 25% of pancreatic tumors contain actionable alterations, of which mutations affecting the deoxyribonucleic acid damage repair (DDR) pathway, such as mutations of *BRCA1* and *BRCA2*, make up the largest part (Pishvaian et al., 2020). Mutations of the DDR pathway specifically disturb the repair of deoxyribonucleic acid (DNA) double-strand breaks by homologous recombination. That explains why tumors with *BRCA* mutations showed an increased sensitivity to DNA crosslinking agents such as platinum and inhibitors of poly-adenosine-diphosphate-ribose polymerase (PARP), an enzyme important for base excision repair (Moffat & O'Reilly, 2020). The POLO trial reported increased progression-free survival rate among patients with a *BRCA1* or *BRCA2* mutation who were treated with the PARP inhibitor olaparib after platinum-based chemotherapy in 1st line (Golan et al., 2019).

Furthermore, in 1% of all PDAC patients and in 10% of *KRAS* wild-type carcinomas, mutations of the protooncogene B-Raf (*BRAF*) can be detected, which affect the mitogen-activated protein kinase (MAPK) signaling pathway (Aguirre et al., 2018). Previous studies reported a sensitivity of *BRAF* mutated pancreatic cancer cell lines to MAPK inhibitors but first application of the MAPK inhibitor trametinib on two pancreatic cancer patients showed controversial results (Aguirre et al., 2018).

Microsatellite instability (MSI) is another potential target for personalized treatment in pancreatic cancer. MSI is caused by deficient mismatch repair genes. Tumors with MSI express an increased amount of mutation-associated neoantigens (MANA) that can be detected by the immune system. In accordance with that, a study of Le et al. treated 12 different tumor entities with MSI, among others pancreatic cancer, with the anti-programmed cell death protein 1 (PD-1) antibody

pembrolizumab and reported radiographic response in 53% and complete response in 21% of patients (Le et al., 2017). This study has led to a Food and Drug Administration (FDA) approval of pembrolizumab for mismatch repair deficient solid tumors progressing after 1st line therapy (Marcus et al., 2019). Notably, MSI occurs at extremely low frequencies of 0.2-0.8% in pancreatic cancer patients, and first clinical studies on pembrolizumab treatment after failure of 1st line therapy showed lower response rates compared to other cancer entities with MSI (Hu et al., 2018; Marabelle et al., 2020).

Though targeted therapies are still an exception in pancreatic cancer management, recent success in identifying targetable mutations represents a significant step towards the implementation of precision medicine in this field.

Thus, the effort increases to simplify access to tumor genomics, aiming to improve the applicability of sequential genotyping to support the development of targeted therapies.

1.3 Liquid Biopsy

The term *Liquid Biopsy* describes the analysis of tumor derived material in body fluids. It allows to gain information on genomic alterations of a tumor and on the prognosis and treatment response of an individual patient by analyzing circulating tumor DNA. These data can be collected by a simple blood sample rather than an invasive biopsy, which means they can be collected more frequently, longitudinally and with less risk for the patient (Crowley et al., 2013). Besides cell-free DNA (cfDNA), other components in the blood were identified carrying information about the underlying tumor, most importantly to be mentioned are circulating tumor cells (CTC), circulating tumor extracellular vesicles and tumor educated platelets (Buscail et al., 2019). Blood is not the only source of tumor derived material suitable for liquid biopsy. Urine, saliva, pleural effusions and cerebrospinal fluid also proved supply of tumor derived information (Corcoran & Chabner, 2018). Since the basis of this thesis is the analysis of cfDNA in pancreatic cancer, further explanations of liquid biopsy will focus on cfDNA, in particular.

1.3.1 Cell-free DNA

Cell-free DNA describes all circulating nucleic acids that can be detected in the noncellular component of the blood and was first reported in plasma by Mandel and Metais (Mandel & Metais, 1948). Since the discovery that the circulating DNA level in the blood stream is elevated among cancer patients, first studies assumed a prognostic and predictive quality in the measurement of circulating DNA level (Leon et al., 1977). Subsequently, several study groups dedicated their work to assess the potential that cfDNA analysis could offer for treatment and diagnostics of cancer. CfDNA is released into the blood stream through apoptosis and necrosis of somatic and cancer cells, but there is also evidence that cells actively shed DNA into circulation, and both mechanisms contribute to the release of nucleic acids into the blood (Jahr et al., 2001; Rogers et al., 1972). Considering the mechanism by which cfDNA is released into the blood, it is not surprising that cfDNA level rises in case of tissue stress such as exercise, inflammation or surgery (Corcoran et al., 2018; Diehl et al., 2008).

Fortunately, tumor specific mutations were detected in cfDNA, suggesting that a part of these molecules is also tumor derived (Sorenson et al., 1994). The part of the cfDNA, carrying tumor specific mutations, is referred to as circulating tumor DNA (ctDNA). The fraction of ctDNA in cfDNA underlies a great variety and ranges from less than 0.1% to more than 90%, depending on tumor type and tumor burden (Corcoran et al., 2018; Diehl et al., 2005; Jahr et al., 2001).

Cell-free DNA is usually double-stranded and fragmented down to a size of more than 400 base pairs, whereas ctDNA shows a higher fragmentation and consists mostly of fragments with a size less than 200 base pairs. The difference in fragment size regarding to the origin of the cfDNA is based on differences in the release mechanisms of the cfDNA into the blood stream (Jahr et al., 2001; Mouliere et al., 2018).

As genetic alterations increasingly influence treatment and diagnostics in cancer management, circulating nucleic acids of the tumor contain valuable information for the understanding of each individual tumor.

1.3.2 Current perspective of ctDNA analysis in cancer

As the attention towards ctDNA analysis arouse, a large number of studies investigated the prognostic value of this biomarker in different cancer entities. Correlation between mutant ctDNA level and disease progression as well as overall survival of patients were observed multiple times (Dawson et al., 2013; Hamana et al., 2005; Schwarzenbach et al., 2012). In accordance with that, the amount of mutant ctDNA correlates with other prognostically relevant parameters such as tumor size, tumor stage and histological grade (Dawson et al., 2013; Schwarzenbach et al., 2012).

CtDNA analysis might even be a better tool to analyze tumor genetics than tissue biopsy (Russo et al., 2016). A disadvantage of the tissue biopsy is its bias to reflect mutational alterations present in a specific part of a tumor without further information on the mutational heterogeneity of all tumor subclones and their metastases (Russo et al., 2016). Studies have found differences in the mutational patterns between metastases and primary tumor as well as in between different tumor lesions, which may explain differences in treatment response between individual tumor lesions (Goyal et al., 2017). Comparing liquid and tissue biopsy, studies reported that ctDNA analysis is able to reflect the mutational heterogeneity detected in multiple tissue biopsies and can reliably detect driver mutations with a 80-90% concordance between ctDNA analysis and tissue biopsy (Blakely et al., 2017; Corcoran et al., 2018; Russo et al., 2016).

In summary, ctDNA detection may offer improvement of prognostic evaluation and diagnostic methods in cancer management and further research in this field is needed.

1.3.3 Implementation of cfDNA analysis in pancreatic cancer

As previously outlined, limited options for early diagnosis and therapy monitoring in the management of pancreatic cancer contribute decisively to its dismal prognosis (Vincent et al., 2011). Initial confirmation of diagnosis and detection of driver mutations is still dependent on an invasive biopsy (Buscail et al., 2019).

For this reason, studies on the value of liquid biopsy in pancreatic cancer have been increasing in number, which are mainly addressing the exploration of ctDNA, CTC, exosomes and cfRNA

(Buscail et al., 2019; Metzenmacher et al., 2020; Zhu et al., 2020). Analysis of CTC and exosomes already revealed promising diagnostic and prognostic value (Yadav et al., 2018). CfRNA detection in pancreatic cancer patients is a less explored area, though first approaches on its value in early diagnosis are promising (Metzenmacher et al., 2020). A main focus of studies on liquid biopsy in pancreatic cancer has been laid on ctDNA testing (Buscail et al., 2019; Zhu et al., 2020).

Because mutations on the *KRAS* gene are a frequently observed event in pancreatic cancer, screening for mutant *KRAS* allows an accurate identification and quantification of the tumor derived proportion of isolated cfDNA (Bailey et al., 2016).

Different methods have been implemented for *KRAS* analysis in cfDNA, which are among others digital droplet polymerase chain reaction (ddPCR), quantitative-PCR, real-time PCR, direct sequencing and next-generation sequencing (NGS) (Buscail et al., 2019). First results of these studies emphasize the potential of ctDNA analysis in diagnostic and prognostic matter. Even in early stages of pancreatic cancer, in which curative treatment is still possible, *KRAS* mutations are detectable by liquid biopsy (Brychta et al., 2016). Furthermore, studies have reported a relation between detectability of ctDNA by mutant *KRAS* analysis and reduced overall survival, progression-free survival (PFS) and disease-free survival after resection (Bernard et al., 2019; Creemers et al., 2017; Hadano et al., 2016; Pietrasz et al., 2017; Sausen et al., 2015). According to some reports, the ctDNA analysis was even able to detect disease recurrence months earlier than the radiological assessment (Sausen et al., 2015; Tjensvoll et al., 2016).

Due to diversity of DNA isolation methods and *KRAS* analysis, comparisons between studies remain difficult (Buscail et al., 2019). More data on the concordance between *KRAS* mutations detectable in the tumor and in plasma are needed when assessing the ability of liquid biopsy to detect tumor mutations (Brychta et al., 2016).

The promising results of previous studies on the benefits of liquid biopsy in pancreatic cancer management inspired this thesis to further explore the feasibility of ctDNA mutant KRAS analysis in PDAC patients.

2 AIMS

This study addressed the urgent need for improvement in advanced pancreatic cancer management. In this sense, it further explored liquid biopsy as a diagnostic and therapeutic option for PDAC patients.

Firstly, different cfDNA isolation methods for ctDNA analysis were evaluated.

Further, a feasibility study was performed in a retrospective design to investigate a possible value of ddPCR mutant *KRAS* detection for prognostic and predictive patient stratification.

Then, these findings were compared with standard methods for prognostic evaluation to see what this method might offer for the treatment of pancreatic cancer.

3 MATERIAL AND METHODS

3.1 Aquisition of patient data

Patients were included into the analysis when either locally advanced or metastatic PDAC was diagnosed and when they were treated with at least one dose of systemic chemotherapy between March 2016 and February 2020. Out of this cohort, patients who had a therapy-naive sampling time point available in the Biobank were analyzed regarding predictive and prognostic value of mutant *KRAS* analysis. Histological diagnosis was based on the current World Health Organization (WHO) criteria and tumor staging was performed according to the AJCC/ UICC TNM classification.

Patients were included from start of 1st line chemotherapy, which they received at the Westdeutsches Tumorzentrum (WTZ). If patients received a resection of the tumor in curative intention and had a relapse, they were included from the day the relapse was diagnosed. The study was approved by the local Ethics Committee of the Medical Faculty of the University Duisburg-Essen (Nr.:17-7729-BO). Data acquisition was performed by retrieving electronic patient files of the hospital platform “Medico”, provided by Cerner Corporation. Using “Medico”, therapy protocols, medical reports, CT images and laboratory results were accessible.

The analysis of chemotherapy application was assisted by the “Computer aided therapy for oncology” (CATO), a software of Becton Dickinson Austria GmbH, which offers precise information about time point of application and dosage of chemotherapeutics. Access to “Medico” and the attached “CATO” were password-protected and the derived data were pseudonymized for further analysis. All data were assembled in an excel table, containing clinicopathological parameters, laboratory values, as well as therapy lines and their corresponding staging results.

3.2 Evaluation of treatment response

Tumor staging was performed every 8-12 weeks depending on the respective chemotherapy protocol by evaluating CT images in accordance with the Response Evaluation Criteria in Solid Tumors (RECIST) version 1.1., which advises to proceed as follows. Potential tumor derived

lesions are distributed into target and non-target lesions. Target lesions measure more than 10 mm in their longest diameter. Five lesions in total and two lesions per organ can be considered as target lesions, referring to multilocular tumor manifestation in one image. Non-target lesions are lymphatic nodes, whose smallest diameter is less than 15 mm, other lesions with longest diameter less than 10 mm, and other unmeasurable manifestations of tumor expansion, such as ascites or blastic bone lesions. Assessing the baseline tumor load in the first CT image is a prerequisite for comparing further staging CT images. For this purpose, the longest diameter of the target lesions, or the smallest diameter in case of lymphatic nodes, is summed to define the tumor load at baseline. In the following staging CT, the previously documented lesions were remeasured, and their variation from baseline tumor burden defined the staging result as presented in the following (Eisenhauer et al., 2009).

Defining Response Criteria based on target lesions (Eisenhauer et al., 2009):

- Complete Response (CR):

  Absolut decline of all target lesions and all pathologically enlarged lymphatic nodes must have a reduction in short axis to < 10 mm.

- Partial Response (PR):

  A minimum of 30% reduction in the sum of diameters of target lesions, taking as reference the baseline tumor load.

- Stable Disease (SD):

  Neither criteria for CR, PR or PD are met.

- Progressive Disease (PD):

  A minimum of 20% increase in the sum of diameters of target lesions, taking as reference the smallest sum on study. Additionally, the increase must be at least 5 mm. The appearance of new lesions during follow-up also defines a progression.

Defining Response Criteria based on non-target lesions (Eisenhauer et al., 2009):

- Complete Response (CR):

  Absolute decline of all non-target lesions along with a normalization of tumor marker level and a shrinkage of all lymphatic nodes down to a size < 10 mm in smallest diameter.

- Not CR/ not PD:

  Maintenance of non-target lesions and/or tumor marker measurable above the normal limits.

- Progressive Disease (PD):

  Unequivocal progression of existing non-target lesions or appearance of new lesions.

Table 2. Evaluating overall response in patients with target and non-target lesions.

Target Lesions	Non-target Lesions	New Lesions	Overall Response
CR	CR	No	CR
CR	Not CR/ not PD	No	PR
CR	Not evaluated	No	PR
PR	Non-PD or not evaluated	No	PR
SD	Non-PD or not evaluated	No	SD
Not all evaluated	Non-PD	No	NE
PD	Any	Yes or No	PD
Any	PD	Yes or No	PD
Any	Any	Yes	PD

3.2.1 Calculation of Overall Survival

Overall Survival (OS) was defined as time from start of 1st assessed chemotherapy until death of any cause. In one case the exact death date was not available so that the patient was censored at the time point of last follow-up. Six patients were alive during the entire observation period and were therefore censored at the 01.02.2020 when the observation ended.

3.2.2 Calculation of Time-to-treatment failure

Time-to-treatment failure (TTF) was defined as time from start of the respective chemotherapy line until last drug administration of the same therapy line. One patient was lost to follow-up during 1st line therapy and was censored at the day the last dose of therapy was administered. Two patients received chemotherapy beyond the end of this study, one during his 1st and one during his 2nd therapy line. These patients were also censored at the end of observation period the 01.02.2020.

3.3 Statistics

The distribution of continuous variables was assigned by mean and median value or interquartile range and standard deviation as appropriate and compared with Wilcoxon test if paired and with Mann-Whitney-U test if unpaired. Categorial variables were summarized as frequency (%) and their deviation was assigned by median and range. The comparison between categorial variables was calculated using Chi-squared test or Fisher's exact test as appropriate.

Overall survival and time-to-treatment failure were calculated using the Kaplan-Meier method (Kaplan & Meier, 1958). The comparison between overall survival and time-to-treatment failure curves was performed using the log-rank test.

The values in figure 15 were logarithmized to simplify representation of small changes in biomarker levels over time and all values were added with 10 to include values of zero in the logarithmized representation.

Statistical analysis was performed using Graph pad prism version eight.

3.4 Methods of the experimental approach

3.4.1 Comparison of cell free DNA isolation Kits

CfDNA yield and fragment size of three commercially available ctDNA isolation kits were compared to find the most suitable method for the liquid biopsy approach. CtDNA is known to be more fragmented in comparison to cfDNA of other origin. As a consequence, the intention was to isolate specifically small DNA fragments (Mouliere et al., 2011). The kits included into the comparison were the Maxwell® RSC ccfDNA Plasma Kit (Promega), QIAmp Circulating Nucleic Acid Kit (QIAGEN) and Zymo Quick-cfDNA™ Serum & Plasma Kit (Zymo Research). The QIAGEN and Zymo kits represent spin column-based methods, whereas the Maxwell RSC kit isolates cfDNA using magnetic beads. The kits were tested each with four samples of 1 ml plasma. The plasma samples are from patients with advanced stage non-small cell lung cancer. An elution volume of 50 µl was set for every kit. The experiments were performed following the manufacturers protocol. The samples were quantified by Quantus™ Fluorometer (Promega),

following the instructions of the company. Subsequently, the fragment length of each sample was measured using the Agilent High Sensitivity D1000 Screen Tape System (Agilent Technologies) regarding to the manufacturers recommendations.

Devices used:

- Maxwell® RSC Instrument (Promega, Madison, WI, USA)
- Quantus™ Fluorometer (Promega, Madison, WI, USA)
- 2200 TapeStation System (Agilent Technologies, Waldbronn, Germany)

Kits used:

- Maxwell® RSC ccfDNA isolation kit (Promega, Madison, WI, USA)
- QIAmp Circulating Nucleic Acid Kit (QIAGEN, Hilden, Germany)
- Quick-cfDNA™ Serum & Plasma Kit (Zymo Research, Irvine, OC, USA)
- QuantiFluor® dsDNA System (Promega, Madison, WI, USA)
- Agilent High Sensitivity D1000 ScreenTape System (Agilent technologies, Waldbronn, Germany)

3.4.2 Blood sampling for mutant *KRAS* detection

Blood was drawn routinely during clinical visits by the responsible hospital staff and plasma was separated by the Westdeutsche Biobank Essen (WBE). According to the Biobank, the separated plasma samples were stored at -80 degrees Celsius until further usage for ddPCR mutant *KRAS* detection.

3.4.3 Next-generation sequencing of primary tumor

Next-generation sequencing (NGS) was performed in the pathology of our clinic. According to their information on the process of the mutation analysis, DNA was isolated from a region of the tumor biopsy containing at least 60% tumor cells. This material was analyzed by NGS of multiple

PCR amplicons. For this purpose, a GeneRead DNAseq Custom Panel V2 (Qiagen), specifically the MAPKtron panel covering 47 genes, was used and a library was generated using NEBNExt® Ultra™ DNA Library Pep Kit from Illumina (NEB). The sequencing was carried out on an Illumina MiSeq™ Machine and the resulting data were analyzed by Cancer Research Workbench (CLC Bio).

3.4.4 DNA isolation

Following the results from the cfDNA isolation kit comparison, the Maxwell® RSC ccfDNA isolation kit (Promega, Madison, WI, USA) was chosen to isolate cfDNA from the plasma of the PDAC cohort. According to the protocol of Maxwell® RSC, all plasma samples were processed as follows: The plasma, previously stored at -80 degrees Celsius, was left for 30 minutes at room temperature to though. In the meantime, prepared cartridges were placed on the deck tray of the Maxwell device, and the sealing foil on top of the cartridges was peeled back. 0.5 ml elution tubes for each isolated DNA sample were labeled and placed into the respective retainer. 1 ml of each plasma sample was transferred into to each well. A plunger was placed into well number eight of each cartridge. 60 µl of elution buffer were added to the bottom of each elution tube and the process was initiated. The isolation results in an elution volume of 50 µl DNA.

Device used:

- Maxwell® RSC Instrument (Promega, Madison, WI, USA)

Kit used:

- Maxwell® RSC ccfDNA isolation kit (Promega, Madison, WI, USA)

Material used:

- Pipettes (Gilson, Madison, WI, USA)
- 0.5 ml PCR Tubes (Promega, Madison, WI, USA)

3.4.5 DNA concentration measurement

The concentration of the eluted DNA was measured using Quantus™ Fluorometer (Promega, Madison, WI, USA), a fluorescence-based method, following the manufacturer's instructions. At first, 20X TE buffer was diluted to 1X TE buffer using nuclease-free water. QuantiFluor® dsDNA Dye working solution was prepared by diluting QuantiFluor® dsDNA dye to 1:200 using 1X TE buffer, and it was kept in foil to stay light protected. All samples including the blank and the standard were prepared in 0.5 ml PCR tubes. Blank was prepared mixing 100 µl working solution and 100 µl 1X TE buffer. For the standard, 2 µl standard DNA, 98 µl 1X TE buffer and 100 µl working solution were mixed. 98 µl of 1X TE buffer and 100 µl working solution were added to 2 µl of each DNA sample. All tubes were vortexed and then kept in the dark for five minutes. Afterwards, DNA concentration of all samples was measured using Quantus™ Fluorometer, ahead of all the blank and the standard to calibrate the device.

Devices used:

- Quantus™ Fluorometer (Promega, Madison, WI, USA)
- Vortex-Genie 2 (Scientific Industries, Bohemia, NY, USA)

Kit used:

- QuantiFluor® dsDNA System (Promega, Madison, WI, USA)

Material used:

- 0.5 ml PCR tubes (Promega, Madison, WI, USA)
- 20X TE-Buffer (Promega, Madison, WI, USA)
- Nuclease-Free Water (Promega, Madison, WI, USA)

3.4.6 Digital droplet PCR mutant *KRAS* detection

The isolated cfDNA was amplified, using digital droplet PCR technology by Bio-Rad (Bio-Rad), which is an emulsion-based method. Using ddPCR™ *KRAS* screening multiplex kit, G12A, G12C,

G12D, G12R, G12S, G12V and G13D *KRAS* mutations can be detected, each with a different assay. The kit contains two TaqMan hydrolysis probes, one specific for the wild-type allele labeled "HEX" and one specific for the *KRAS* mutant allele labeled "FAM" and a single primer pair for each assay. The positive control was DNA from A549, an alveolar adenocarcinoma derived cell line, which contains homozygous mutated *RAS* at the protein sequence G12S (Giard et al., 1973). As negative control served DNA from DIFI, a colorectal carcinoma derived cell line which contains homozygous wild-type *RAS* gene (Untawale et al., 1993). Following the manufacturer's protocol, duplicates for each DNA sample were prepared in a 96-well plate, mixing 5 µl of sample, 11 µl of ddPCR Supermix for Probes (No dUTP), 4.9 µl of nuclease-free water and 1.1 µl of multiplex primers and probes, adding up to a total volume of 22 µl per sample. Because the amount of ctDNA in each sample is not reflected by the DNA concentration measured, equal volumes of each sample were taken to further proceed with ddPCR amplification, regardless of their respective DNA concentrations. To generate the droplets, 20 µl of each sample were transferred into a DG8™ cartridge (Bio-Rad) and 70 µl of Droplet Generation Oil for Probe (Bio-Rad) were added to the respective row. The cartridges were covered with a DG8™ Gasket (Bio-Rad) and droplets were generated using QX100 Droplet Generator (Bio-Rad). Afterwards, 40 µl of droplets were transferred into another 96-well plate, covered with pierceable Foil Heat Seal (Bio-Rad) and sealed with a PX1 PCR plate sealer (Bio-Rad). After the sealing process, the 96-well plate was transferred into the thermal cycler and the DNA was amplified according to the cycling conditions recommended by the manufacturer (table 3).

Table 3. Cycling conditions for PCR amplification.

Cycling Step	Temperature (°C)	Time	Ramp Rate	Number of Cycles
Enzyme activation	95	10 min	2 °C/s	1
Denaturation	94	30 s	2 °C/s	40
Annealing/extension	Optimum	1 min	2 °C/s	40
Enzyme deactivation	98	10 min	2 °C/s	1
Hold	4	infinite	1 °C/s	1

Following the amplification process, absolute quantification of positive and negative droplets was performed by the QX100™ Droplet Reader (Bio-Rad) and analyzed with QuantaSoft™ Software Version 1.7.4. (Bio-Rad). The positive endpoint was defined as detection of a droplet containing one of the seven detectable *KRAS* mutations. The results of the analysis were calculated in number of positive copies per 1 ml of plasma. The thresholds were set based on the positive and negative controls in each run and were set around 7.000 for channel 1 (FAM) and 3.000 for channel 2 (HEX).

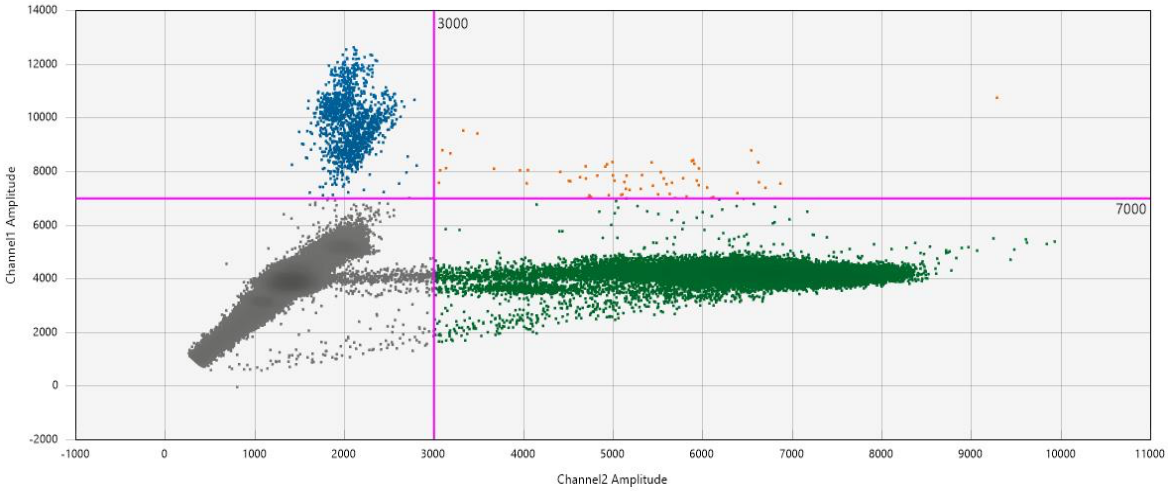

Figure 1. Two-dimensional scatterplot showing the fluorescence amplitude of channel 1 (FAM) and channel 2 (HEX) for each droplet.

Thresholds were set at 7.000 for channel 1 and 3.000 for channel 2. In blue color: FAM positive droplets containing *KRAS* mutant DNA. In green color: HEX positive droplets containing *KRAS* wild-type DNA. In orange color: FAM and HEX positive droplets, containing *KRAS* mutant and *KRAS* wild-type DNA. In grey color: FAM and HEX negative droplets, containing no measurable *KRAS* gene sequence.

Devices used:

- PX1™ PCR Plate sealer (Bio-Rad, Hercules, CA, USA)
- SensoQuest LabCycler (Sensoquest, Göttingen, Germany)
- QX100™ droplet reader (Bio-Rad, Hercules, CA, USA)

Kits used:

- ddPCR™ *KRAS* Screening Multiplex Kit (Bio-Rad, Hercules, CA, USA)

Material used:

- DNA from A549
- DNA from DIFI
- DdPCR™ 96-Well Plate (Bio-Rad, Hercules, CA, USA)
- Nuclease-free water, Aqua B. Braun (B.Braun, Melsungen, Hessen, Germany)
- DG8™ cartridge (Bio-Rad, Hercules, CA, USA)
- Droplet Generator Oil (Bio-Rad, Hercules, CA, USA)

- DG8™ Gasket (Bio-Rad, Hercules, CA, USA)
- Pierceable Foil Heat Seal (Bio-Rad, Hercules, CA, USA)
- Pipettes (Gilson, Madison, WI, USA)

4 RESULTS

The present study investigated the options circulating mutant *KRAS* analysis may offer in the management of pancreatic cancer.

First, the qualitative and quantitative performance of different commercially available cell-free DNA (cfDNA) isolation kits was evaluated in order to select the best performing kit.

CfDNA was then isolated from plasma samples and mutant *KRAS* load in each sample was determined by means of droplet digital PCR (ddPCR).

Subsequently, clinical data, including therapy and patient's response, were analyzed.

Further, mutant *KRAS* detection in blood and tumor biopsy were correlated with survival data and compared with established methods for response monitoring such as CT imaging and CA 19-9 levels.

4.1 Evaluation of DNA isolation methods for liquid biopsy

The isolation of high quality cfDNA is an indispensable first step to allow a precise evaluation of the ctDNA analysis in the following.

For this purpose, we evaluated the performance of different commercially available cfDNA isolation kits. Tumor-derived DNA is typically shorter than genomic DNA in circulation, which leads to the assumption that the kit with the highest yield of small DNA fragments would be preferable (Mouliere et al., 2018). The Qiagen kit, which is frequently used in many studies on liquid biopsy, was compared with the Zymo and the Maxwell kit.

The Qiagen kit showed the highest DNA yield with an average of 20.6 ng/ml plasma, compared to the Maxwell and Zymo kits, which reached an average DNA yield of 10.4 ng and 10.9 ng, respectively (table 4).

Table 4. CfDNA yield isolated by three different cfDNA isolation kits.

DNA was isolated by each kit from four plasma samples. Each sample consisted of 1 ml of plasma and derived from non-small cell lung cancer patients. The Qiagen kit recovered the highest DNA yield, compared to the Maxwell and the Zymo kits.

Kit	Mean DNA yield ng/ml plasma	Standard Deviation	No. of Samples
Maxwell	10.4	+/- 8.3	4
Zymo	11	+/- 8.4	4
Qiagen	20.6	+/- 3.9	4

Additionally, the size distribution of the isolated DNA was analyzed on the TapeStation using the High sensitivity D1000 DNA ScreenTape Analysis. This analysis showed that the Maxwell kit exclusively isolated smaller DNA fragments with a length around 160-200 bp. The Qiagen and the Zymo kits recovered both small DNA fragments with a length of 160-200 bp and large DNA fragments with a length of 500-600 bp (table 5, figure 2).

Table 5. TapeStation analysis of DNA fragment length.

The isolated fragments can be divided into two size ranges from 160-200 bp and from 500-600 bp. The Maxwell kit only isolated small fragments. The Qiagen kit recovered more large fragments than small fragments, whereas the Zymo kit isolated more small fragments than large fragments.

Fragment range	Maxwell (pg/µl)	Zymo (pg/µl)	Qiagen (pg/µl)
	Mean (SD)	Mean (SD)	Mean (SD)
160-200 bp	48.6 (+/- 61.51)	55.75 (+/- 75.4)	12.4 (+/- 13)
500-600 bp	0	14.3 (+/- 10.3)	40.6 (+/- 26.8)

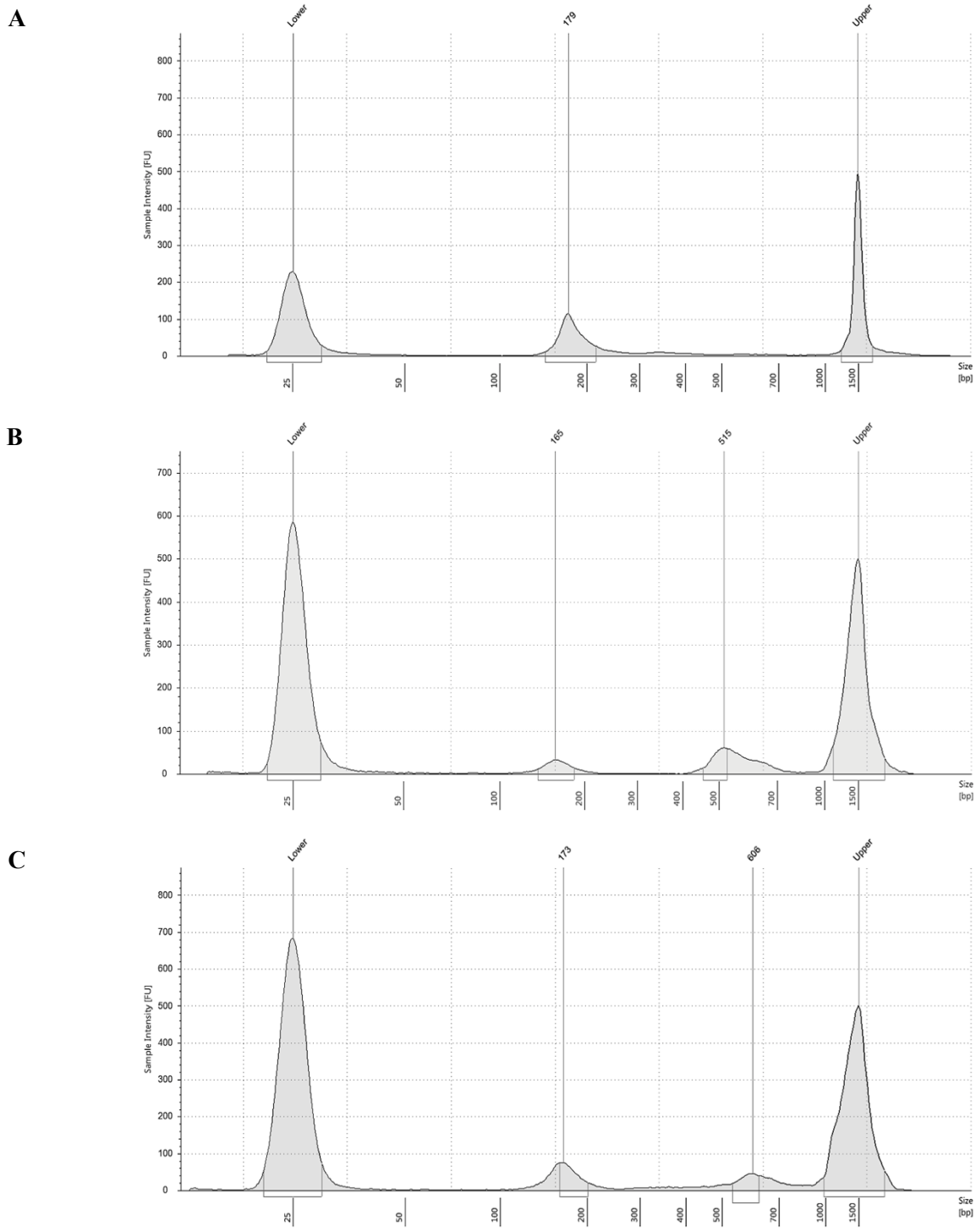

Figure 2. Electrophoretic view of TapeStation runs, analyzing cfDNA size profiles.

Size profiles of the isolated DNA fragments were obtained by TapeStation runs. **A:** The fragment length isolated by the Maxwell kit covered a range of 160-210 bp with a mean length of 179 bp. **B:** The Qiagen kit recovered two size ranges of DNA fragments, one with a mean length of 515 and a range of 420-700 and a smaller fraction with a mean length of 165 and a range of 150-200. **C:** The two size ranges isolated by the Zymo kit show one larger fraction with a mean length of 172 and a range of 150-210 and one smaller fraction with a mean length of 606 and a range of 500-1000.

These results demonstrate that the Maxwell kit was able to isolate a purer fraction of small-fragmented DNA, whereas the Zymo and the Qiagen kit additionally recovered larger DNA fragments. This finding was crucial for the decision to perform DNA isolation with the Maxwell kit within the further course of this study. A noteworthy advantage of the Maxwell kit is its ability to self-sterilize after each sample prep which helps to avoid contaminations.

4.2 Detection of mutant *KRAS* in cell-free DNA by ddPCR

4.2.1 Assessing the limit of detection for the ddPCR approach

At the beginning, detection limits of mutant *KRAS* by ddPCR were assessed. Therefore, homozygote mutant *KRAS* DNA was serial diluted in wild-type DNA. The dilution range covered dilutions from 1:10 to 1:20000 and in this setting, a limit of detection (LoD) of 1:500 was determined.

4.2.2 Mutant *KRAS* detection in healthy patient plasma

In addition to that, the detectability of mutant *KRAS* DNA in the plasma of healthy patients was performed and the average detectable amount of mutant *KRAS* in these patients was 8 copies/ml plasma. Based on these findings, mutant *KRAS* copies above 8 copies/ml were defined as cut-off value for mutant *KRAS* positive samples.

4.2.3 Patient selection for mutant *KRAS* detection

A cohort of 65 patients diagnosed with pancreatic ductal adenocarcinoma and treated between the beginning of 2016 and the beginning of 2019 were eligible for this study. As a precondition for the ddPCR experiments it was assured that blood samples from all patients were available in the biobank. The study was focused on late-stage pancreatic ductal adenocarcinoma to maximize chances of mutant *KRAS* detection, consequently nine patients were excluded based on their UICC stage (UICC < III). Four patients were treated in an external clinic and could not be enrolled into the study due to incomplete data assessment by the external physicians. Another set of three

patients were excluded because they received chemotherapy according to the protocol of the "AIO NEOLAP" study which would falsify the evaluation of treatment and follow-up data as treatment decisions were made independent of tumor behavior (figure 3). Finally, blood samples of 49 patients were used for ddPCR analysis. Histopathological features, most frequently described to influence detection rates of mutant *KRAS*, are summarized in table 6. Additionally, clinico-oncological characteristics of the same patient cohort are shown in table 7.

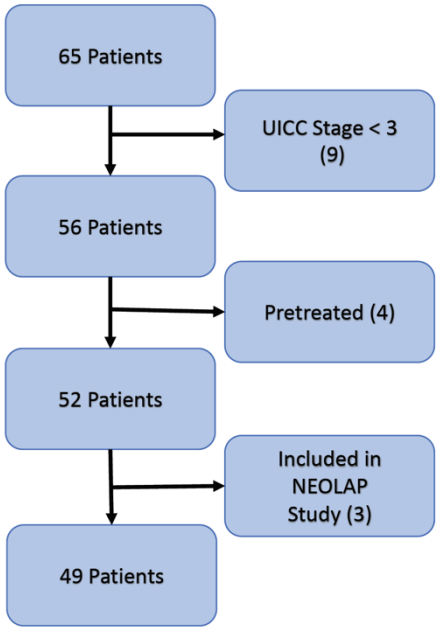

Figure 3. CONSORT diagram describing patient selection of our study cohort.
Patient selection was performed based on availability of blood samples in the biobank and UICC stage. Pretreated patients and patients included into the NEOLAP study were excluded from the analysis (Kunzmann et al., 2021). From an initial cohort of 65 patients, 49 patients were selected for this study.

Table 6. Histopathological features for all 49 patients selected for the liquid biopsy approach.

Abbreviations: UICC stage: Union for International Cancer Control, TNM stage according to the 7th UICC/AJCC edition.

Variable	Patient cohort for treatment analysis (N=49)
UICC stage	
III	6.1% (N=3)
IV	93.9% (N=46)
Grading	
G1	4.1% (N=2)
G2	59.1% (N=29)
G3	32.7% (N=16)
Gx	4.1% (N=2)
T-stage	
T2	20.4% (N=10)
T3	26.5% (N=13)
T4	20.4% (N=10)
Tx	32.7% (N=16)
N-stage	
N0	12.2% (N=6)
N1	28.6% (N=14)
N2	4.1% (N=2)
Nx	55.1% (N=27)
M-stage	
M0	6.1% (N=3)
M1	93.9% (N=46)
Sites of metastasis	
hepatic	71.4% (N=35)
peritoneal	32.7% (N=16)
pulmonary	20.4% (N=10)
other	20.4% (N=10)
Number of metastatic sites	
1	59.2% (N=29)
> 1	34.7% (N=17)
Primary tumor location	
head	51% (N=25)
body or tail	49% (N=24)

Table 7. Clinico-oncological features of the *KRAS* detection cohort.

Biomarker levels refer to the treatment-naive sampling time point. **Abbreviations:** ECOG: Eastern Cooperative Oncology Group, BORR: Best Overall Response Rate, LDH: Lactate dehydrogenase, CRP: C-reactive protein, CA 19-9: Carbohydrate antigen 19-9, CTX: chemotherapy, Gem: gemcitabine, 5-FU: 5-fluorouracil.

Variable	Patient cohort for treatment analysis (N=49)
Gender	
male	65.3% (N=32)
female	34.7% (N=17)
Age in years	
Median	61
Range	37-82
25^{th} ; 75^{tho}%ile	55 ; 66
≥ 60 years	55.1% (N=27)
≥ 70 years	14.3% (N=7)
≥ 75 years	4.1% (N=2)
ECOG pre CTX	
0	69.4% (N=34)
1	16.3% (N=8)
2 or more	14.3% (N=7)
Lines of therapy	
received 1 line	100% (N=49)
received 2 lines	36.7% (N=18)
received 3 or more lines	10.2% (N=5)
1^{st} line therapy	
5-FU-based	67.3% (N=33)
Gem-based	32.7% (N=16)
2^{nd} line therapy	
5-FU-based	22.2% (N=4/18)
Gem-based	77.8% (N=14/18)
1^{st} line CTX 5-FU-based BORR	
PR	39.4% (N=13/33)
SD	42.4% (N=14/33)
PD	18.2% (N=6/33)
NC	0% (N=0/33)
n.a.	0% (N=0/33)
1^{st} line CTX Gem-based BORR	
PR	25% (N=4/16)
SD	37.5% (N=6/16)
PD	25% (N=4/16)
NC	6.3% (N=1/16)
n.a.	6.3% (N=1/16)

LDH > 240 (U/l) ULN		
	> 240 (U/l)	57.1% (N=28)
	< 240 (U/l)	42.9% (N=21)
	Median (U/l)	250
	25^{th} ; 75^{th}%ile (U/l)	202 ; 298
CRP > 0.5 (mg/dl) ULN		
	> 0.5 (mg/dl)	83.7% (N=41)
	< 0.5 (mg/dl)	16.3% (N=8)
	Median (mg/dl)	2.5
	25^{th} ; 75^{th}%ile (mg/dl)	0.8 ; 4.4
CA 19-9 > 37 (U/ml) ULN		
	> 37 (U/ml)	83.7% (N=41)
	< 37 (U/ml)	16.3% (N=8)
	Median (U/ml)	6981.4
	25^{th} ; 75^{th}%ile (U/ml)	351.5 ; 27907

4.2.4 Results of ddPCR mutant *KRAS* analysis

DNA isolation and mutant *KRAS* detection was performed for all eligible patients. Accordingly, a set of 125 plasma samples, from the 49 patients enrolled in this study, was profiled with ddPCR. The median cfDNA concentration of these samples was 15.5 ng/ml plasma (IQR: 9.5-73 ng/ml). Mutant *KRAS* was detectable in 58.4% of samples (n=73/152) with a median mutant *KRAS* load of 69 copies/ml plasma (IQR: 18-500 copies/ml). A therapy-naive sampling time point (T0) was available from 32 patients in this cohort and from 22 patients, at least one follow-up time point was available after start of chemotherapy. The amount of mutant *KRAS* positive patients, as well as the median number of mutant *KRAS* copies/ml was lower after therapy started (50% vs 65.6% and 32 copies/ml vs 180 copies/ml). The mutational allele fraction (MAF) was calculated for both groups, which describes the ratio between mutant *KRAS* counts and the sum of wild-type *KRAS* and mutant *KRAS* counts. T0 samples presented higher MAF values with a median of 6.15% (IQR: 1.04-20.35), compared with the posttreatment samples with an MAF of 0.37% (IQR: 0.28-1.6) (table 8).

Table 8. Results of DNA isolation and ddPCR mutant *KRAS* analysis from patient plasma.

The results of ddPCR mutant *KRAS* analysis are presented in three groups: once the results for all patients and all follow-up samples analyzed (N=49) and separately the results of the therapy-naive sampling time point (N=32) and the first posttreatment time point (N=22). **Abbreviations:** conc.: concentration, T0: therapy-naive sampling time point, T1: first time point after treatment, MAF: mutational allele fraction.

Variable		All patients (N=49)	T0 (N=32)	T1 (N=22)
No. of samples		n=125	n=32	n=22
CfDNA conc. (ng/ml)				
	Median (ng/ml)	15.5	13.7	18.8
	Range (ng/ml)	2-800	3.3-800	2-180
	25^{th} ; 75^{th}%ile (ng/ml)	9.5 ; 73	9.2 ; 25.8	7.7 ; 53
***KRAS* status**				
	KRAS^{mut} positive	58.4% (n=73/125)	65.6% (n=21/32)	50% (n=11/22)
	KRAS^{mut} negative	41.6% (n=52/125)	34.4% (n=11/32)	50% (n=11/22)
***KRAS*^{mut} positive samples (copies/ml)**				
	Median (copies/ml)	69	180	32
	Range (copies/ml)	10-118200	14-118200	14-500
	25^{th} ; 75^{th}%ile (copies/ml)	18 ; 500	66 ; 1260	16 ; 48
MAF of *KRAS*^{mut} positive samples (%)				
	Median (%)	1.22	6.15	0.37
	Range (%)	0.03-60.93	0.35-60.93	0.09-3.3
	25^{th} ; 75^{th}%ile (%)	0.37 ; 8.25	1.04 ; 20.35	0.28 ; 1.6

4.3 Analysis of treatment and follow-up data of the patient cohort

The results of this study must be interpreted in the context of any inconsistencies between this patient cohort and other study populations.

For this purpose, treatment and follow-up data of the patient cohort were closely analyzed and coherences between patient characteristics and survival data were examined.

4.3.1 Selection of palliative chemotherapy regimen in the study cohort

The optional therapy regimens can be divided into therapies that are based on 5-FU as therapeutic drug and those based on gemcitabine. The majority of patients in this cohort received a 5-FU-based therapy as 1st line treatment (N=33), whereas 16 patients received a gemcitabine-based therapy as primary treatment (N=16). The 5-FU-based therapy group consisted of 30 cases which received the combination of 5-FU, irinotecan, oxaliplatin and folinic acid (FOLFIRINOX) and three cases treated with the combination of 5-FU, folinic acid and oxaliplatin (FOLFOX). A combination of gemcitabine and nab-paclitaxel was administered in 12 out of 16 gemcitabine-based first line therapies. The remaining patients (N=4) were treated with gemcitabine alone.

2nd line treatment was feasible for 18 patients and various treatment regimens were selected for that purpose, including FOLFIRINOX, FOLFOX, the Napoli-protocol, gemcitabine nab-paclitaxel and gemcitabine monotherapy. Because of the various distribution of 2nd line treatments, correlations between individual 2nd line regimen and outcome would have a low statistical power. Thus, the focus of this analysis laid on the 1st line therapy (figure 4).

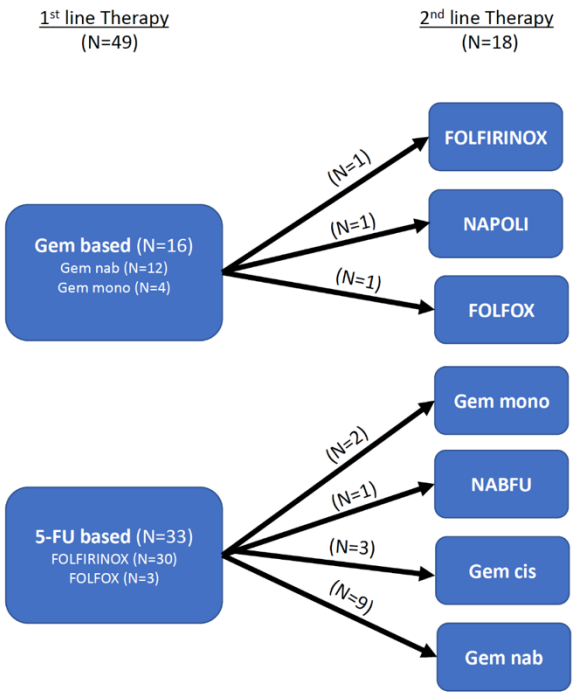

Figure 4. Treatment distribution within 1st and 2nd line therapy administered in the study cohort.

Within the cohort of 49 patients, 16 patients were treated with a gemcitabine-based regimen and 33 patients received a 5-FU-based treatment as 1st line. A 2nd line was feasible for 18 patients. **Abbreviations:** Gem: Gemcitabine, nab: nab-paclitaxel, FOLFIRINOX: Folinic acid, 5-FU, irinotecan, oxaliplatin, FOLFOX: Folinic acid, 5-FU, oxaliplatin, cis: cisplatin, NABFU: Nab-paclitaxel, folinic acid, 5-FU, NAPOLI: nanoliposomal irinotecan, 5-FU, folinic acid.

4.3.2 Comparison of patient characteristics between the two treatment arms

In the following, the histopathological and clinico-oncological characteristics of the patients were compared depending on whether a 5-FU- or gemcitabine-based treatment was administered as 1st line. This helped to identify a potential bias between the two therapy groups, which might affect survival and treatment response (table 9,10).

Table 9. Histopathological features divided according to 1st line treatment.

P-values were generated by fisher's exact test and were placed in the respective row of the parameter that was compared to the other parameters of this category. **Abbreviations:** UICC stage: Union for International Cancer Control, TNM stage according to the 7th UICC/AJCC edition.

Variable		5-FU-based (N=33)	Gemcitabine-based (N=16)	p-value
UICC stage				
	III	6.1% (N=2)	6.3% (N=1)	> 0.99
	IV	93.9% (N=31)	93.8% (N=15)	
Grading				
	G1	6.1% (N=2)	0% (N=0)	
	G2	57.6% (N=19)	62.5% (N=10)	
	G3	30.3% (N=10)	37.5% (N=6)	0.75
	Gx	6.1% (N=2)	0% (N=0)	
T-stage				
	T2	24.2% (N=8)	12.5% (N=2)	
	T3	24.2% (N=8)	31.3% (N=5)	
	T4	21.2% (N=7)	18.8% (N=3)	> 0.99
	Tx	30.3% (N=10)	37.5% (N=6)	
N-stage				
	N0	15.2% (N=5)	6.3% (N=1)	
	N1	33.3% (N=11)	18.8% (N=3)	
	N2	6.1% (N=2)	0% (N=0)	> 0.99
	Nx	45.5% (N=15)	75% (N=12)	
M-stage				
	M0	6.1% (N=2)	6.3% (N=1)	
	M1	93.9% (N=31)	93.8% (N=15)	
Sites of metastasis				
	hepatic	66.7% (N=22)	81.3% (N=13)	0.62
	peritoneal	30.3% (N=10)	37.5% (N=6)	
	pulmonary	24.2% (N=8)	12.5% (N=2)	
	other	21.2% (N=7)	18.8% (N=3)	
Number of metastatic sites				
	1	60.6% (N=20)	56.3% (N=9)	> 0.99
	> 1	33.3% (N=11)	37.5% (N=6)	
Primary tumor location				
	head	51.5% (N=17)	50% (N=8)	> 0.99
	body or tail	48.5% (N=16)	50% (N=8)	

Table 10. Clinico-oncological features divided according to the 1st line treatment.

P-values were generated by Fisher's exact test or by Mann-Whitney-U test as appropriate and were placed in the respective row of the parameter that was compared to the other parameters of this category. Biomarker levels refer to the treatment-naive sampling time point. **Abbreviations:** ECOG: Eastern Cooperative Oncology Group, LDH: Lactate dehydrogenase, CRP: C-reactive protein, CA 19-9: Carbohydrate antigen 19-9, CTX: chemotherapy, 5-FU: 5-fluorouracil.

Variable		5-FU-based (N=33)	Gemcitabine-based (N=16)	p-value
Gender				
	male	60.6% (N=20)	75% (N=12)	0.36
	female	39.4% (N=13)	25% (N=4)	
Age in years				
	Median	58	65.5	**0.007**
	Range	37-73	49-82	
	25th ; 75th%ile	55 ; 63	60 ; 72.25	
	≥ 60 years	(N=14)	(N=13)	
	≥ 70 years	(N=2)	(N=5)	
	≥ 75 years	(N=0)	(N=2)	
ECOG pre CTX				
	0	69.7% (N=23)	68.8% (N=11)	
	1	15.2% (N=5)	18.8% (N=3)	
	2 or more	15.2% (N=5)	12.5% (N=2)	> 0.99
Lines of therapy				
	received 1 line	100% (N=33)	100% (N=16)	0.39
	received 2 lines	45.5% (N=15)	18.8% (N=3)	
	received 3 or more lines	14.3% (N=4)	6.3% (N=1)	
LDH > 240 (U/l) ULN				
	> 240 (U/l)	54.5% (N=18)	62.5% (N=10)	
	< 240 (U/l)	45.5% (N=15)	37.5% (N=6)	
	Median (U/l)	269	247	0.59
	25th ; 75th%ile (U/l)	197 ; 308	211.75 ; 267.25	
CRP > 0.5 (mg/dl) ULN				
	> 0.5 (mg/dl)	78.8% (N=26)	93.8% (N=15)	
	< 0.5 (mg/dl)	21.2% (N=7)	6.3% (N=1)	
	Median (mg/dl)	2	2.65	0.95
	25th ; 75th%ile (mg/dl)	0.8 ; 5	1.75 ; 3.53	
CA 19-9 > 37 (U/ml) ULN				
	> 37 (U/ml)	84.8% (N=28)	81.3% (N=13)	
	< 37 (U/ml)	15.2% (N=5)	18.8% (N=3)	
	Median (U/ml)	5614.15	6981.4	0.99
	25th ; 75th%ile (U/ml)	342.4 ; 33514.32	741.6 ; 20562	

4.3.3 Survival analysis

Follow-up was performed until the 01.02.2020. At data lock, six patients were still alive and one patient was lost to follow-up, so they were censored at last day of follow-up. Median follow-up time of the censored patients was 15.7 months. The longest overall survival observed in this study was 27.2 months and the shortest was 1.9 months. The median overall survival of all 49 patients was 9.4 months (figure 5).

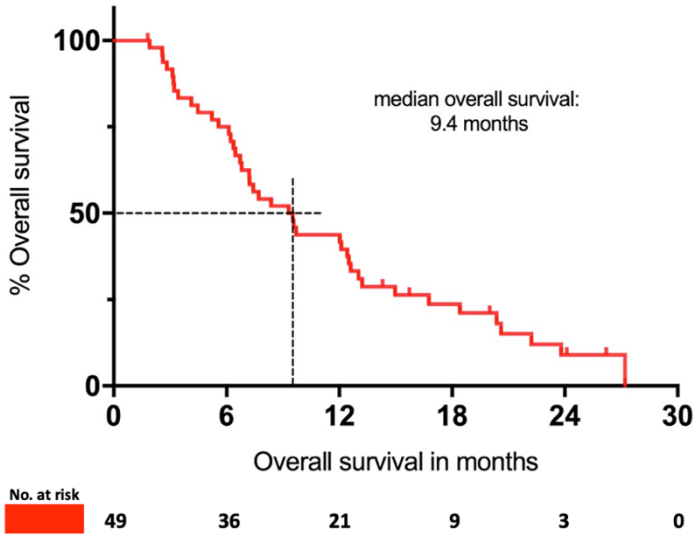

Figure 5. Kaplan-Meier analysis illustrating the overall survival of the patient cohort.
Median overall survival of the patient cohort (N=49) was 9.4 months. The shortest survival period was 1.9 months and the longest survival period was 27.2 months.

Furthermore, time-to-treatment failure (TTF) of 1st and 2nd line treatments was calculated. Because a 2nd line therapy was not administered in all cases, the TTF of the 1st line was calculated as follows. In the first setup all patients were pooled, regardless of if they were subjected to a 2nd line treatment or not (N=49) (figure 6A). In addition, those patients who underwent a 2nd line treatment were analyzed, exclusively (N=18) (figure 6B).

Comparing the median TTF of the 1st line for all patients (N=49) with the group of patients who received a 2nd line treatment, revealed a 1.2 month longer TTF for the second group (4.9 months vs 6.1 months). This might be because the 1st group includes more patients who had to end the 1st line

treatment prematurely due to a deterioration of the general condition and did not recover enough to receive a 2nd line treatment. The median TTF of the 1st line was for both patient groups with 4.9 months (N=49) and 6.1 months (N=18) significantly longer compared to the 2nd line which showed a median TTF of 2.1 months (figure 6).

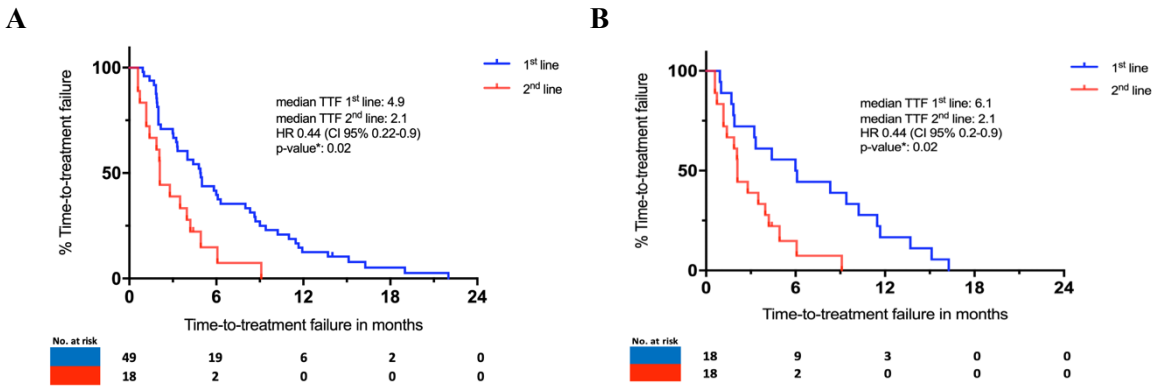

Figure 6. Kaplan-Meier curves comparing TTF of 1st and 2nd line treatment.

A: Overview of all patients, who received a 1st line therapy (N=49). Median TTF of the 1st line therapy was with 4.9 months significantly longer than the TTF of the 2nd line with 2.1 months (p-value*: 0.011, log-rank test). The hazard ratio was 0.44 (CI 95% 0.22-0.9) **B:** In this graph, only those patients who received a 2nd line were included into the evaluation of the 1st line (N=18). The median TTF of the 1st line was 6.1 months, compared to 2.1 months for the 2nd line which was also statistically significant (p-value*:0.02, log-rank test). The hazard ratio was 0.44 (CI 95% 0.2-0.9).

In the following, clinical features were analyzed regarding their correlation with the follow-up data of the study cohort. In this context, OS was more than two times higher for patients with an Eastern Cooperative Oncology Group (ECOG) status of 0 (12.4 months), compared with patients with an ECOG status of 1 (5.6 months) (p-value*: 0.009, log-rank test) (figure 7A). A similar trend could be observed for the relation between ECOG status and TTF. Patients with an ECOG status of 0 had a median TTF of 6 months, which is 2.2 times longer compared to the median TTF of patients with an ECOG of 1 (2.7 months) (p-value*: 0.028, log-rank test) (figure 7B).

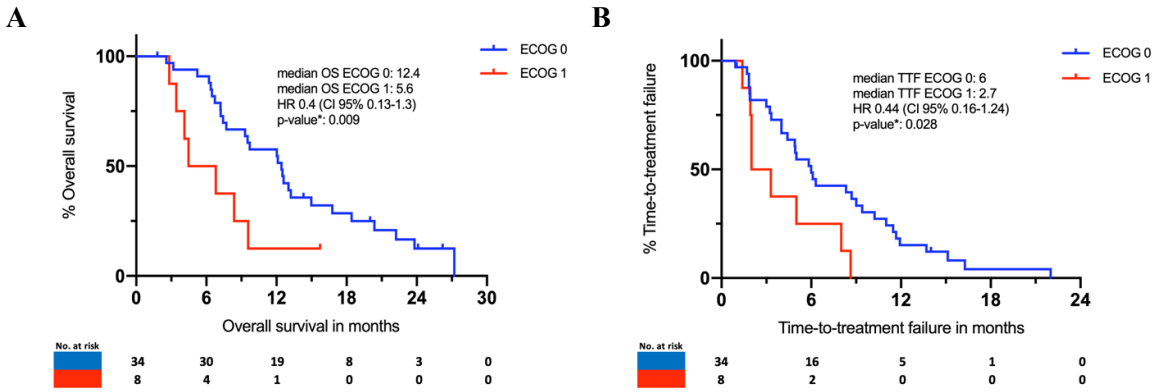

Figure 7. Impact of the ECOG status on overall survival and treatment response of PDAC patients.

A: Comparison between ECOG status and overall survival (N=42). An ECOG status of 0 was associated with a significantly longer median OS (12.4 months vs 5.6 months) compared to patients with an ECOG status of 1 (p-value*: 0.009, log-rank test). The hazard ratio was 0.4 (CI 95% 0.13-1.3). **B:** Comparison between ECOG status and TTF (N=42). Patients with ECOG 0 showed a 3.3 months longer median TTF compared to patients with ECOG 1 (6 months vs 2.7 months, p-value*: 0.028, log-rank test). The hazard ratio of the two patient groups was 0.44 (CI 95% 0.16-1.24).

To examine whether the choice of 1st line treatment was associated with a better outcome, the therapy protocols were divided into 5-FU- and gemcitabine-based protocols and compared afterwards.

Median OS of the 5-FU-based treatment was 9.6 months, which was slightly longer than the 6.4 months OS observed in the gemcitabine-based therapy arm (figure 8A).

The TTF was similar in both treatment groups with a median of 5 months for the 5-FU-based therapies and 4.85 months for the gemcitabine-based therapies (figure 8B). The differences between the two therapy groups were statistically not significant neither concerning the OS (p-value: 0.84, log-rank test) nor the TTF (p-value: 0.21, log-rank test).

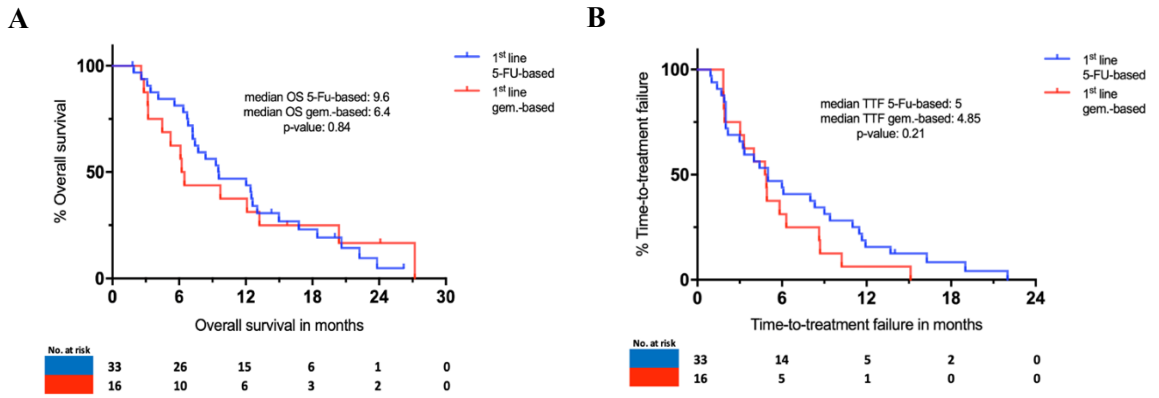

Figure 8. Kaplan-Meier analysis comparing survival and treatment response depending on the 1st line treatment.

A: OS of patients with a 5-FU-based 1st line therapy and patients with a gemcitabine-based 1st line therapy (N=49). OS was 9.6 months for 5-FU-based and 6.4 months for gemcitabine-based therapy, respectively (p-value: 0.84, log-rank test). **B:** TTF of patients with a 1st line 5-FU-based therapy compared to a gemcitabine-based 1st line therapy (N=49). Median TTF was 5 months for a 5-FU-based regimen and 4.89 months for gemcitabine-based treatments (p-value: 0.21, log-rank test).

4.4 Evaluation of the prognostic and predictive value of mutant *KRAS*

To explore the value of mutant *KRAS* as a prognostic biomarker and its behavior in the blood during therapy, estimation of baseline levels in terms of a therapy-naive sampling time point (T0) was warranted. The patient selection was adapted for that purpose, and 32 patients with a T0 time point were included into this analysis (figure 9).

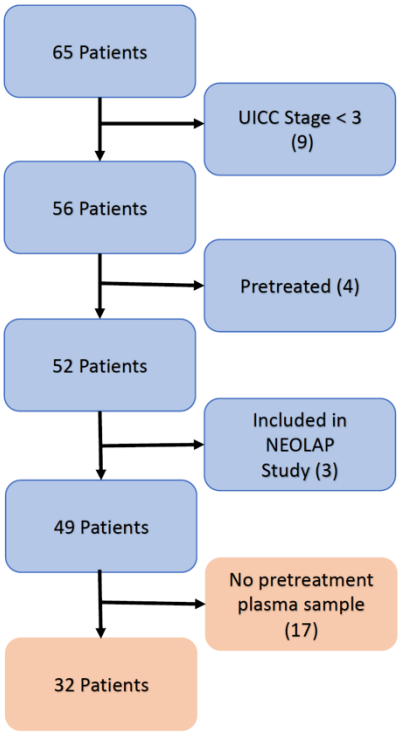

Figure 9. CONSORT diagram illustrating the inclusion of patients for ddPCR analysis.
To analyze the prognostic value of mutant *KRAS* detection, 17 patients had to be excluded from the investigation because no pretreatment plasma sample was available. Therefore, the final analysis was carried out with 32 patients.

Both histopathological and clinico-oncological features of the patient cohort with T0 sampling time points were compared to those of the original cohort (N=49) and appeared comparable (table 11,12). Accordingly, it can be assumed that the T0 patient cohort is a representative selection of the overall 49 patients enrolled in this study.

Table 11. Histopathological features of the *KRAS* detection cohort.

Abbreviations: UICC stage: Union for International Cancer Control, 7. TNM Classification according to UICC/AJCC.

Variable	Patient cohort for ddPCR analysis (N=32)
UICC stage	
III	6.3% (N=2)
IV	93.8% (N=30)
Grading	
G1	3.1% (N=1)
G2	56.3% (N=18)
G3	34.4% (N=11)
Gx	6.3% (N=2)
T-stage	
T2	25% (N=8)
T3	28.1% (N=9)
T4	15.6% (N=5)
Tx	31.3% (N=10)
N-stage	
N0	6.3% (N=2)
N1	31.3% (N=10)
N2	6.3% (N=2)
Nx	56.3% (N=18)
M-stage	
M0	6.3% (N=2)
M1	93.8% (N=30)
Sites of metastasis	
hepatic	75% (N=24)
peritoneal	28.1% (N=9)
pulmonary	25% (N=8)
other	15.6% (N=5)
Number of metastatic sites	
1	59.4% (N=19)
> 1	34.4% (N=11)
Primary tumor location	
head	43.8% (N=14)
body or tail	56.3% (N=18)

Table 12. Clinico-oncological features of the *KRAS* detection cohort.

Biomarker levels refer to the treatment-naive sampling time point. **Abbreviations:** ECOG: Eastern Cooperative Oncology Group, BORR: Best Overall Response Rate, LDH: Lactate dehydrogenase, CRP: C-reactive protein, CA 19-9: Carbohydrate antigen 19-9, CTX: chemotherapy, Gem: gemcitabine, 5-FU: 5-Fluorouracil.

Variable	Patient cohort for ddPCR analysis (N=32)
Gender	
male	68.8% (N=22)
female	31.3% (N=10)
Age in years	
Median	61.5
Range	45-80
25^{th} ; 75^{th}%ile	55.8 ; 67.3
≥ 60 years	56.3% (N=18)
≥ 70 years	18.8% (N=6)
≥ 75 years	3.1% (N=1)
ECOG pre CTX	
0	75% (N=24)
1	12.5% (N=4)
2 or more	12.5% (N=4)
Lines of therapy	
received 1 line	100% (N=32)
received 2 lines	40.6% (N=13)
received 3 or more lines	12.5% (N=4)
1^{st} line therapy	
5-FU-based	75% (N=24)
Gemcitabine-based	25% (N=8)
2^{nd} line therapy	
5-FU-based	23.1% (N=3/13)
Gemcitabine-based	76.9% (N=10/13)
1^{st} line CTX 5-FU-based BORR	
PR	37.5% (N=9/24)
SD	41.7% (N=10/24)
PD	20.8% (N=5/24)
NC	0% (N=0/24)
n.a.	0% (N=0/24)
1^{st} line CTX Gem-based BORR	
PR	25% (N=2/8)
SD	50% (N=4/8)
PD	25% (N=2/8)
NC	0% (N=0/8)
n.a.	0% (N=0/8)

LDH > 240 (U/l) ULN		
	> 240 (U/l)	56.3% (N=18)
	< 240 (U/l)	43.8% (N=14)
	Median (U/l)	250.5
	25^{th} ; 75^{th}%ile (U/l)	204.5 ; 289.5
CRP > 0.5 (mg/dl) ULN		
	> 0.5 (mg/dl)	84.4% (N=27)
	< 0.5 (mg/dl)	15.6% (N=5)
	Median (mg/dl)	2,95
	25^{th} ; 75^{th}%ile (mg/dl)	0.98 ; 5
CA 19-9 > 37 (U/ml) ULN		
	> 37 (U/ml)	78.1% (N=25)
	< 37 (U/ml)	21.9% (N=7)
	Median (U/ml)	12845
	25^{th} ; 75^{th}%ile (U/ml)	351.5 ; 27907

Furthermore, clinicopathological features of T0 mutant *KRAS* positive and T0 mutant *KRAS* negative patients were compared to identify differences between the two subgroups. This comparison showed that the number of cases with hepatic metastasis and Lactate dehydrogenase (LDH) and CA 19-9 level were higher in mutant *KRAS* positive patients (Table 13,14).

Table 13. Histopathological features of mutant *KRAS* positive and negative patients.

P-values were generated by Fisher's exact test and were placed in the respective row of the parameter that was compared to the other parameters of this category. Biomarker levels refer to the treatment-naive sampling time point. **Abbreviations:** UICC stage: Union for International Cancer Control, 7. TNM Classification according to UICC/AJCC.

Variable		T0 *KRAS* + (N=21)	T0 *KRAS* - (N=11)	p-value
UICC stage				
	III	4.8% (N=1)	9.1% (N=1)	> 0.99
	IV	95.2% (N=20)	90.9% (N=10)	
Grading				
	G1	4.8% (N=1)	0% (N=0)	
	G2	52.4% (N=11)	63.6% (N=7)	
	G3	38.1% (N=8)	27.3% (N=3)	0.7
	G n.a.	4.8% (N=1)	9.1% (N=1)	
T-stage				
	T2	23.8% (N=5)	27.3% (N=3)	> 0.99
	T3	19% (N=4)	45.5% (N=5)	
	T4	19% (N=4)	9.1% (N=1)	
	T n.a.	38.1% (N=8)	18.2% (N=2)	
N-stage				
	N0	4.8% (N=1)	9.1% (N=1)	> 0.99
	N1	28.6% (N=6)	36.4% (N=4)	
	N2	4.8% (N=1)	9.1% (N=1)	
	N n.a.	61.9% (N=13)	45.5% (N=5)	
M-stage				
	M0	4.8% (N=1)	9.1% (N=1)	
	M1	95.2% (N=20)	90.9% (N=10)	
Sites of metastasis				
	hepatic	90.5% (N=19)	45.5% (N=5)	**0.04**
	peritoneal	19% (N=4)	45.5% (N=5)	
	pulmonary	14.3% (N=3)	54.5% (N=6)	
	other	19% (N=4)	9.1% (N=1)	
Number of metastatic sites				
	1	61.9% (N=13)	54.5% (N=6)	> 0.99
	> 1	33.3% (N=7)	36.4% (N=4)	
Primary tumor location				
	head	42.9% (N=9)	45.5% (N=5)	> 0.99
	body or tail	57.1% (N=12)	54.5% (N=6)	

Table 14. Clinico-oncological features of mutant *KRAS* positive and negative patients.

P-values were generated by Fisher's exact- or Mann-Whitney-U test as appropriate and were placed in the row of the parameter that was compared to the other parameters. Biomarker levels refer to the treatment-naive time point. **Abbreviations:** ECOG: Eastern Cooperative Oncology Group, BORR: Best Overall Response Rate, LDH: Lactate dehydrogenase, CRP: C-reactive protein, CA 19-9: Carbohydrate antigen 19-9, CTX: chemotherapy, 5-FU: 5-Fluorouracil, Gem: gemcitabine.

Variable		T0 *KRAS* + (N=21)	T0 *KRAS* - (N=11)	p-value
Gender				
	male	57.1% (N=12)	90.9% (N=10)	0.11
	female	42.9% (N=9)	9.1% (N=1)	
Age in years				
	Median	62	61	0.51
	Range	45-80	48-69	
	25^{th} ; 75^{tho}%ile	56 ; 71	56 ; 64.5	
	≥ 60 years	57.1% (N=12)	54.5% (N=6)	
	≥ 70 years	28.6% (N=6)	0% (N=0)	
	≥ 75 years	4.8% (N=1)	0% (N=0)	
ECOG pre CTX				
	0	71.4% (N=15)	81.8% (N=9)	0.52
	1	14.3% (N=3)	9.1% (N=1)	
	2 or more	14.3% (N=3)	9.1% (N=1)	
Lines of therapy				
	received 1 line	100% (N=21)	100% (N=11)	0.9
	received 2 lines	42.9% (N=9)	36.4% (N=4)	
	received ≥ 3 lines	4.8% (N=1)	27.3% (N=3)	
1^{st} line therapy				
	5-FU-based	71.4% (N=15)	81.8% (N=9)	0.68
	Gem-based	28.6% (N=6)	18.2% (N=2)	
2^{nd} line therapy				
	5-FU-based	22% (N=2/9)	25% (N=1/4)	
	Gem-based	78% (N=7/9)	75% (N=3/4)	
1^{st} line CTX 5-FU-based BORR				
	PR	46.7% (N=7/15)	22.2% (N=2/9)	0.34
	SD	40% (N=6/15)	44.4% (N=4/9)	
	PD	13.3% (N=2/15)	33.3% (N=3/9)	0.24
	NC	0% (N=0/15)	0% (N=0/9)	
	n.a.	0% (N=0/15)	0% (N=0/9)	
1^{st} line CTX Gem-based BORR				
	PR	0% (N=0/6)	100% (N=2/2)	
	SD	66.7% (N=4/6)	0% (N=0/2)	
	PD	33.3% (N=2/6)	0% (N=0/2)	
	NC	0% (N=0/6)	0% (N=0/2)	
	n.a.	0% (N=0/6)	0% (N=0/2)	

LDH > 240 (U/l) ULN				
	> 240 (U/l)	71.4% (N=15)	27.3% (N=3)	
	< 240 (U/l)	28.6% (N=6)	72.7% (N=8)	
	Median (U/l)	273	207	**0.009**
	25^{th} ; 75^{th}%ile (U/l)	226 ; 298	173 ; 228.5	
CRP > 0.5 (mg/dl) ULN				
	> 0.5 (mg/dl)	85.7% (N=18)	81.8% (N=9)	
	< 0.5 (mg/dl)	14.3% (N=3)	18.2% (N=2)	
	Median (mg/dl)	3.4	2.8	0.96
	25^{th} ; 75th%ile (mg/dl)	1.1 ; 4.4	0.9 ; 7.65	
CA 19-9 > 37 (U/ml) ULN				
	> 37 (U/ml)	76.2% (N=16)	81.8% (N=9)	
	< 37 (U/ml)	23.8% (N=5)	18.2% (N=2)	
	Median (U/ml)	22183.6	351.5	**0.002**
	25^{th} ; 75^{th}%ile (U/ml)	8799 ; 101162	201 ; 554	

4.4.1 Prognostic value of mutant *KRAS* compared to CA 19-9

The prognostic value of the established biomarker CA 19-9 was compared to mutant *KRAS* levels before therapy (T0), to further assess the value of a liquid biopsy approach in clinical routine. Patients with a pretreatment CA 19-9 level below 37 U/ml were excluded from the analysis, as a discrimination of non-producers from low CA 19-9 levels is not possible based on the available data. The remaining 16 patients were evaluated regarding a possible association between mutant *KRAS* values in copies/ml plasma and CA 19-9 level in U/ml. This analysis revealed a positive trend between elevated CA 19-9 values and mutant *KRAS* levels (Spearmen correlation coefficient: > 0.5), the strength of this relationships was however moderate (Mukaka, 2012) (figure 10).

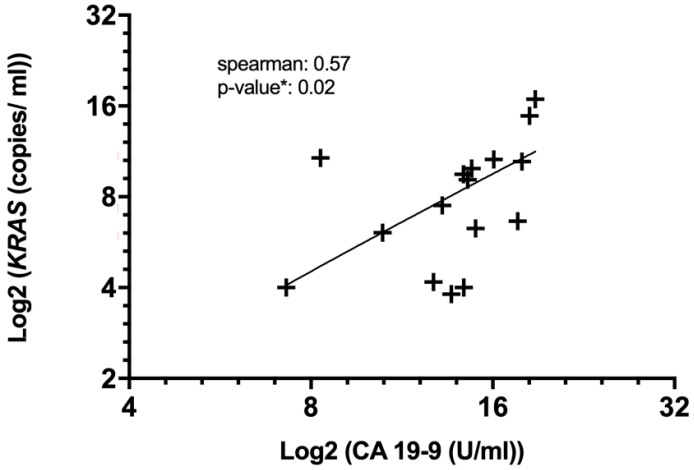

Figure 10. Correlation between elevated CA 19-9 and mutant *KRAS* positive levels (N=16). CA 19-9 values above 37 U/ml and elevated mutant *KRAS* level were logarithmized and plotted against each other on this graph. The Spearman correlation coefficient was: r=0.57 (p-value*: 0.0224).

To allow a comparison between elevated CA 19-9 and mutant *KRAS* levels, a cut-off value between high and low levels of the respective parameter is required. Therefore, CA 19-9 levels, mutant *KRAS* positive levels, as well as the MAF of *KRAS* were illustrated on a histogram, to visualize the distribution of these values. A cut-off value of 3162 U/ml was used to distinguish high CA 19-9 levels from low levels because it lays in the middle between a peak in the high CA 19-9 level range and a peak in the low CA 19-9 level range as the histogram illustrates (figure 11A). The median of 180 copies/ml plasma was chosen to distinguish between high and low mutant *KRAS* level (figure 11B). Furthermore, a cut-off value of 1.5% was set to separate high and low MAF values (figure 11C).

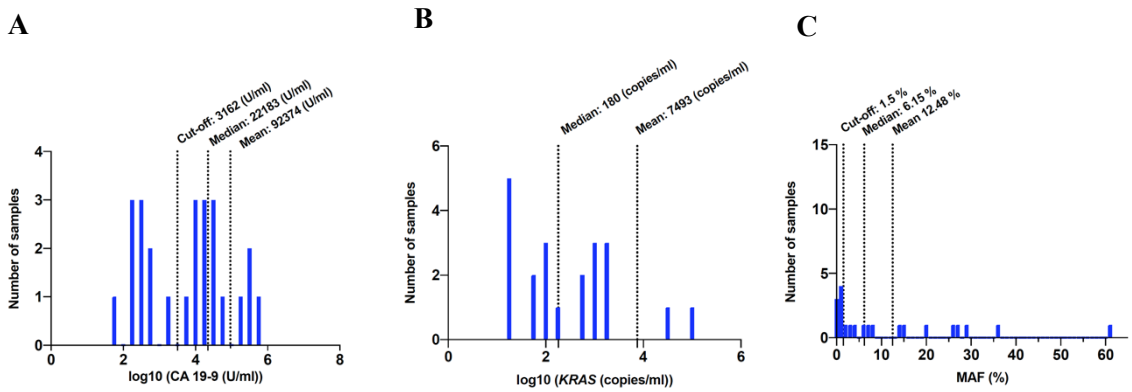

Figure 11. Distribution of CA 19-9, mutant *KRAS* and MAF.

Logarithmized CA 19-9 and mutant *KRAS* levels as well as MAF of mutant *KRAS* were plotted on a histogram to visualize the distribution of the values. **A:** Elevated CA 19-9 levels were separated in high and low levels using the cut-off 3162 U/ml (N=25). **B:** The median of 180 copies/ml is suitable to separate Mutant *KRAS* positive counts in high and low levels (N=21). **C:** MAF (%) were divided into high and low MAF using the cut-off 1.5% (N=21).

Next, Kaplan-Meier analysis was performed to analyze which one of the four parameters: CA 19-9, mutant *KRAS* positivity, absolute mutant *KRAS* level in copies/ml plasma or mutant *KRAS* calculated as MAF, would correlate best with the overall survival. Patients with CA 19-9 levels below 3162 U/ml had a significantly higher median OS (18.2 months), compared to patients with CA 19-9 levels above 3162 U/ml (7.5 months) (p-value*: 0.024, HR 0.36, CI 95% 0.15-0.9, log-rank test) (figure 12A). The analogues comparison of mutant *KRAS* levels observed a 1.36 times longer median OS when mutant *KRAS* was not detectable at baseline (median OS 9.3 months vs 12.6 months, p-value*: 0.037, HR 0.41, CI 95% 0.18-0.9, log-rank test) (figure 12B).

A distribution of mutant *KRAS* values using the cut-off 180 copies/ml plasma, resulted in no significant difference in median OS (median OS 8.6 months vs 9.3 months, p-value: 0.11, HR 0.54, CI 95% 0.23-1.3, log-rank test) (figure 12C). Patients with a MAF of less than 1.5% at baseline showed a 1.5 times longer median OS compared to patients with a baseline MAF above that cut-off (median OS 8.3 vs 12.6, p-value*: 0.027, HR 0.43, CI 95% 0.19-0.97, log-rank test) (figure 12D).

The calculation of mutant *KRAS* values as MAF showed the best correlation with the overall survival from the three analyzed variations to describe mutant *KRAS* data at baseline. Overall, CA

19-9 divided by the cut-off 3162 U/ml illustrated the best correlation with overall survival in this scenario (figure 12).

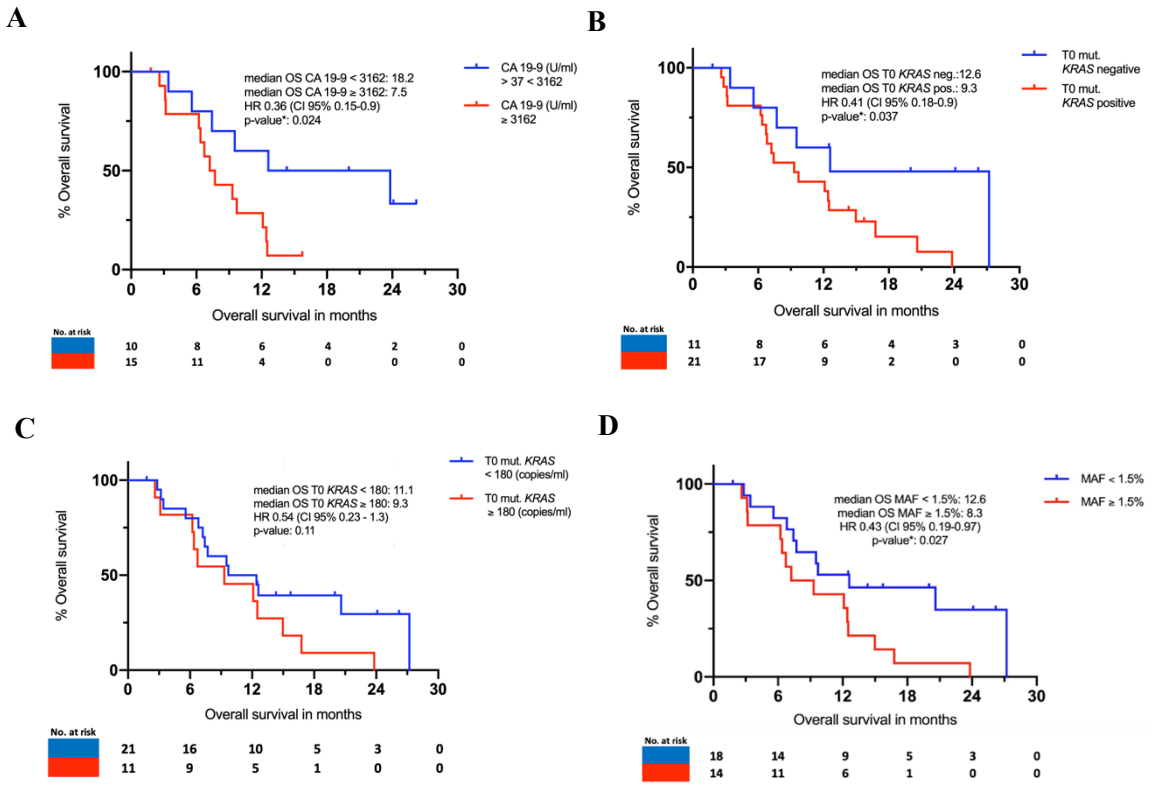

Figure 12. Predictive value of mutant *KRAS* and CA 19-9 on overall survival.

A: Patients with CA 19-9 ≥ 3162 at baseline showed a significantly shorter median OS (7.5 vs 18.2 months, N=25, p-value*: 0.024, HR 0.54, CI 95% 0.23-1.3, log-rank test). **B:** Detectable mutant *KRAS* at baseline was associated with a reduced median OS (12.6 vs 9.3, N=32, p-value*: 0.037, HR 0.41, CI 95% 0.18-0.9, log-rank test). **C:** Median OS was longer for patients with low mutant *KRAS* level (N=32, p-value: 0.11, HR 0.54, CI 95% 0.23-1.3, log-rank). **D:** A MAF below 1.5% was associated with a longer median OS (12.6 vs 8.3 months, N=32, p-value*: 0.027, HR 0.43, CI 95% 0.19-0.97, log-rank test).

In addition, the above analyzed parameters were studied for their correlation with TTF. Patients with a baseline CA 19-9 value below 3162 U/ml showed a 6.2 months longer median TTF, compared to patients with higher CA 19-9 level (10.2 months vs 4 months, p-value*: 0.018, HR 0.43, CI 95% 0.19-0.99, log-rank test) (N=25) (figure 13A).

The TTF of patients without measurable mutant *KRAS* at baseline was 1.43 times longer than for mutant *KRAS* positive patients (TTF 6.3 months vs 4.4 months, p-value: 0.61, HR 0.83, CI 95% 0.39-0.73, log-rank test) (figure 13B).

Patients with a mutant *KRAS* level below 180 copies/ml plasma showed a slightly prolonged TTF of 6.4 months, compared to 4.4 months for patients with mutant *KRAS* values below this cut-off (p-value: 0.64, HR 0.84, CI 95% 0.39-1.81, log-rank test) (figure 13C).

The analysis of MAF at baseline revealed that initially those patients with an MAF ≥ 1.5% presented a longer TTF and shortly after 50% of patient experienced treatment failure, the event ratio reversed and now patients with an MAF < 1.5% took more time until failure of the 1st line treatment. The log-rank test for these curves indicated that the difference between the two groups was statistically not significant (p-value: 0.31) (figure 13D).

Overall, CA 19-9 was the only one from the four parameters that correlated significantly with the TTF.

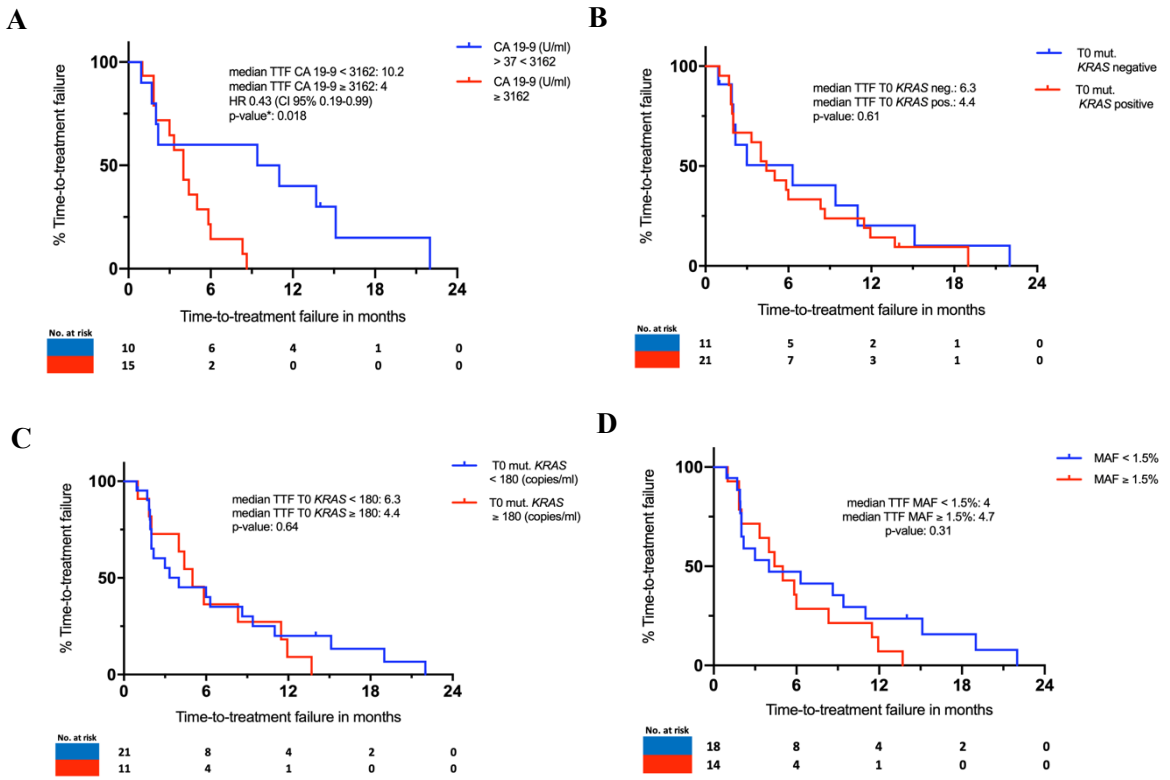

Figure 13. Kaplan-Meier analysis of mutant *KRAS* and CA 19-9 at baseline in correlation to TTF.

A: Patients with a CA 19-9 ≥ 3162 at baseline showed a significantly shorter median TTF (10.2 vs 4 months, N=25, p-value*: 0.018, HR 0.43, CI 95% 0.19-0.99, log-rank test). **B:** Detectability of mutant *KRAS* at baseline was not associated with a difference in TTF (6.3 vs 4.4, N=32, p-value: 0.61, log-rank test). **C:** Patients with high mutant *KRAS* level did not show a difference in TTF, compared to patients with low mutant *KRAS* level (N=32, p-value: 0.64, log-rank test). **D:** MAF below or above the cut-off 1.5% was not associated with a significant difference in TTF (4 vs 4.7 months, N=32, p-value: 0.31, log-rank test).

4.4.2 Correlation of mutant *KRAS* status with the best-overall-response-rate

In the following, it was analyzed if the presence of mutant *KRAS* at baseline correlates with the best-overall-response-rate (BORR). Specifically, a Chi-square test was performed, which compared patients with partial response to patients with stable disease or progressive disease as BORR regarding their baseline mutant *KRAS* status.

This analysis could not detect a correlation between mutant *KRAS* status and BORR (p-value: 0.864, chi-square) (figure 14, table 15).

Table 15. Fourfold table of the chi-square test comparing response rate and detectability of mutant *KRAS*.

The best overall-response-rate (BORR) was divided into two categories: once patients that reached a partial regression (PR) and secondly the patients that either reached a stable disease (SD) or progressive disease (PD.) These categories were further subdivided regarding their mutant *KRAS* status at baseline to form a fourfold table for the chi-square analysis. The distribution of BORR of patients with and without detectable mutant *KRAS* at baseline did not show a different treatment response depending on the detectability of mutant *KRAS* at baseline.

BORR	No. of mutant *KRAS* positive patients	No. of mutant *KRAS* negative patients
PR	7	4
SD	10	4
PD	4	3

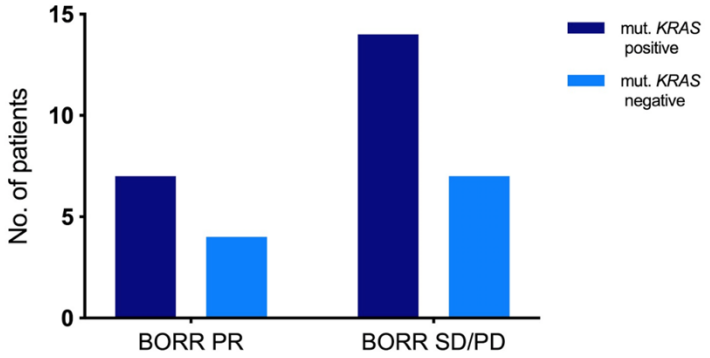

Figure 14. Bar chart illustrating mutant *KRAS* at baseline and the corresponding best-overall-response rate of the patient.

Patients were divided in two groups depending on their treatment response. One group contained patients that showed a partial response (PR) and those patients with stable disease (SD) or progressive disease (PD). From this, a chi-square analysis was performed that did not support a correlation between BORR and mutant *KRAS* status (p-value: 0.864, N=32, chi-square test).

4.4.3 Analysis of mutant *KRAS* detection and CT-imaging in individual patients

One aspect of this work was, to evaluate the ability of the cfDNA mutant *KRAS* level to monitor the clinical course of the patients in our cohort. Therefore, mutant *KRAS* levels of longitudinal liquid biopsy samples from patients with at least three follow-up time points were plotted as a

function of time together with the corresponding CA 19-9 values. The criteria for this analysis were met by eight patients of which two were excluded as they were still alive and have not experienced disease progression until the end of study. CT-based imaging results were used as benchmark for the clinical course of the tumor burden. All mutations detectable in the tumor tissue of the respective patient are listed above each graph. In all of the six patients the mutant *KRAS* level was detectable before start of 1st line therapy (range: 100-1750 copies/ml) and the mutant *KRAS* level dropped down after chemotherapy started (range: 0-500 copies/ml). From these examples, patient 11 (**A**), 13 (**B**) and 5 (**C**) showed a rise in mutant *KRAS* level before a CT morphologic progress was detected. In the case of patient 11 and 13, the rise in mutant *KRAS* was accompanied by increasing CA 19-9 values. The CA 19-9 level of patient 5 also increased, but the respective blood sample was drawn after the CT scan was made (**C**). Mutant *KRAS* levels of patient 64 (**D**) and 2 (**E**) also correlated with the radiological tumor progress, however not prior to the CT results. Out of the six cases analyzed, patient 68 (**F**) is the only case in which the dynamic in *KRAS* level did not correlate with the tumor behavior. In fact, mutant *KRAS* dropped despite of a CT morphologic tumor progress (**F**). Overall, in five of the six patients, mutant *KRAS* detection correlated with the disease monitoring by CT and CA 19-9. In three of these patients, the mutant *KRAS* analysis detected disease progress earlier than the CT. Mutant *KRAS* analysis failed to detect disease progression in one of the six examples (figure15).

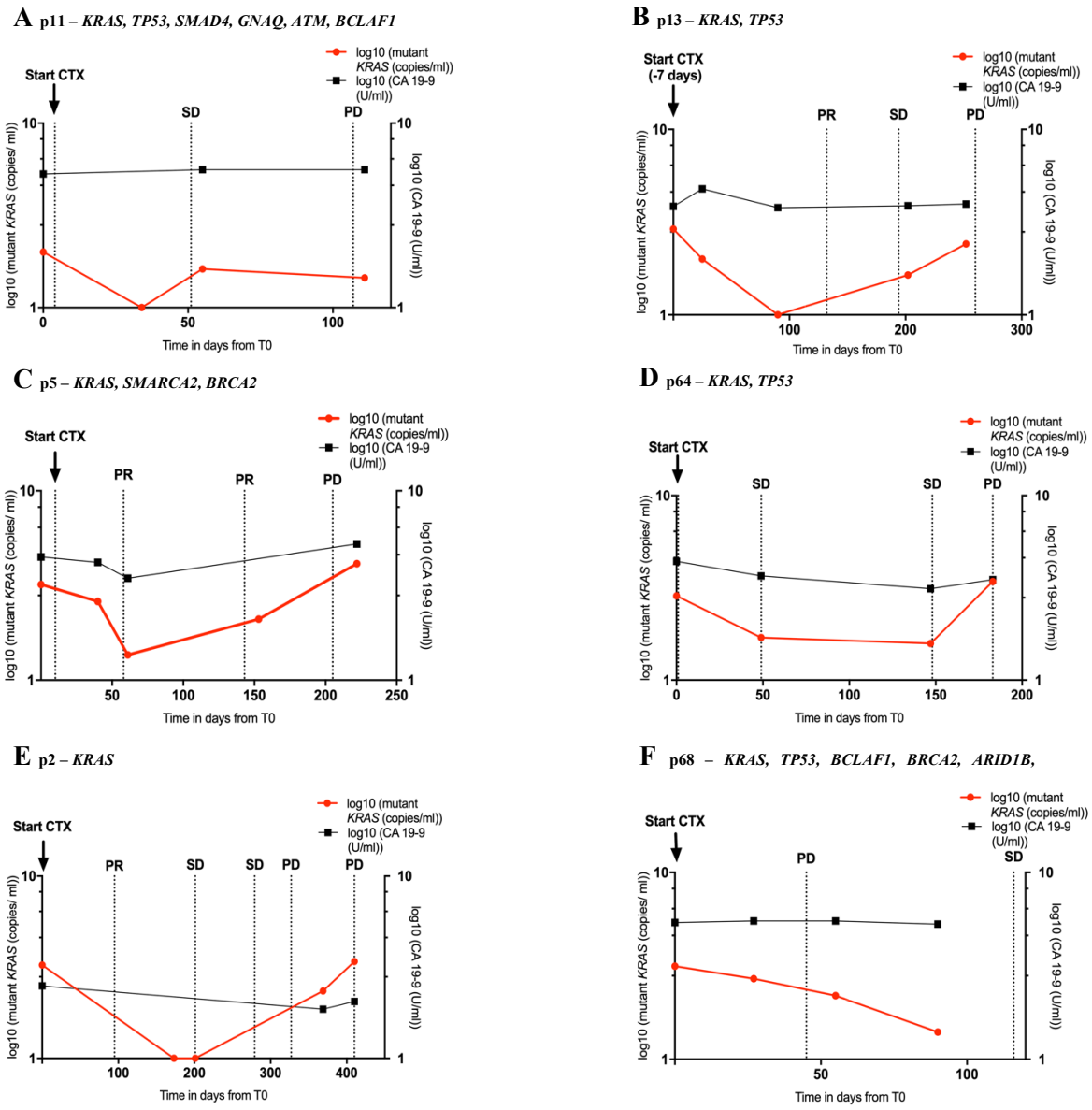

Figure 15. Dynamic behavior of mutant *KRAS* and CA 19-9 level in relation to CT-based response evaluation criteria in solid tumors (RECIST) under treatment.

The heading of each graph names the code for the individual patient along with the mutations detected within the respective tumor. $KRAS^{mut}$ and CA 19-9 levels were logarithmized and plotted as a function of time to visualize their dynamics during treatment. All values were added with 10 to allow values of zero in the logarithmized representation. The start of chemotherapy (CTX) cycle is marked in every graph. In the case of patient 13 (B), the start of therapy was 7 days before the first biomarker level was assessed. Dotted lines mark the CT- staging time points and are labeled with the corresponding staging results: partial regression (PR), stable disease (SD), progressive disease (PD), according to the RECIST criteria.

4.4.4 Prognostic value of changes in *KRAS* status during therapy

As next step, I explored if changes in mutant *KRAS* detectability after initiation of therapy are associated with a certain prognosis. I divided patients with blood samples available from the time point before and after start of 1st line, in three groups (N=18). Group one contains patients who showed measurable mutant *KRAS* before initiating 1st line therapy and dropped down to no measurable mutant *KRAS* at the 1st time point after start of therapy. These seven patients were classified as therapy responders. The 2nd group describes patients who presented measurable mutant *KRAS* before and at the 1st time point after the start of 1st line therapy. These patients were called non-responders referring to the persistently measurable mutant *KRAS* after start of chemotherapy. Furthermore, in five patients mutant *KRAS* was neither measurable before initiating therapy nor at the 1st time point after initiating therapy. They define group three and classify patients with low tumor activity. Only follow-up time points within 50 days from therapy start were considered (table 16).

Table 16. Overall survival and treatment response depending on the changes of mutant *KRAS* level after start of palliative treatment.

Three groups were formed depending on the mutant *KRAS* behavior before and after treatment onset. Group one marked the therapy responders, group two the non-responders and group three described the patients with low tumor activity. Median OS and TTF were calculated by Kaplan-Meier analysis.

	Group 1	**Group 2**	**Group 3**
Change of mutant *KRAS*	T0 pos./T1 neg.	T0 pos./T1pos.	To neg./T1 neg.
No. of patients	7	6	5
Median OS (months)	16.8	12.3	27.2
Median TTF 1st line (months)	8.6	5.9	10.2

In the following, a Kaplan-Meier analysis was performed on OS and TTF data of responders and non-responders. A median OS of 16.8 months and a median TTF of 8.6 months was observed for the responders, whereas the non-responders had a shorter OS and TTF of 12.3 and 5.9, respectively

(OS: p-value: 0.29, HR 0.55, CI 95% 0.16-1.83, log-rank test), (TTF: p-value: 0.6, HR 0.76, CI 95% 0.24-2.38, log-rank test), (figure 16).

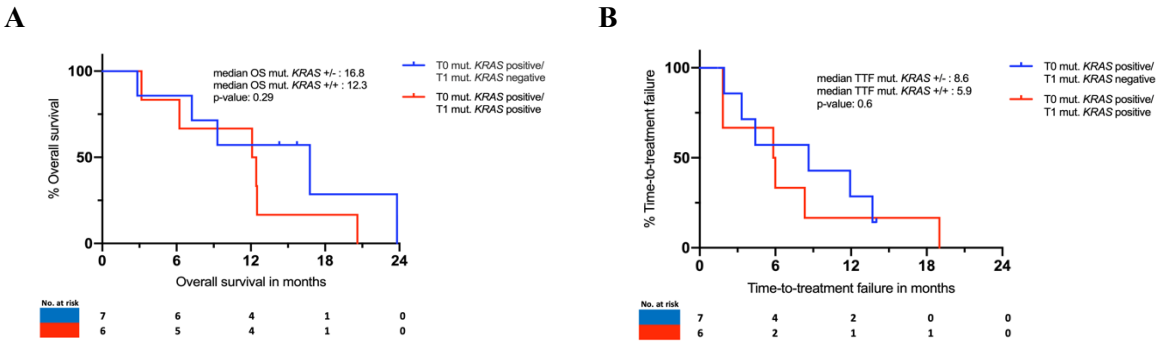

Figure 16. Kaplan-Meier graphs comparing survival and treatment response of responders and non-responders.

A: Treatment responders showed a 4.5 months longer median OS than non-responders (16.8 vs 12.3 months), (p-value: 0.29, log-rank test), (N=13). **B**: Treatment responders showed a 2.7 months longer median TTF than non-responders (8.6 months vs 5.9 months), (p-value: 0.6, log-rank test), (N=13).

In addition to that, follow-up data of group three and group two were analyzed and compared with the previously presented analysis of the mutant *KRAS* status at baseline to investigate if continuous mutant *KRAS* detection after treatment onset is more informative than the baseline mutant *KRAS* detection alone (figure 17). Patients with low tumor activity (group three) showed a significantly longer OS (27.2 months), compared with the non-responders (group two) (12.3 months) (p-value*: 0.016, HR 0.19, CI 95% 0.04-0.82). The hazard ratio of the analysis including the follow-up time point is lower compared to the hazard ratio of the baseline $KRAS^{mut}$ analysis (0.19 vs 0.41). Therefore, in this analysis the difference in survival rates increases when both time points are included into the analysis.

This finding does not apply to the TTF. Even though, Kaplan-Meier curves separate better when considering both pre and post therapy mutant *KRAS* status, the curves cross at about 15 months follow-up. Accordingly, no significant difference can be assessed neither for this comparison (p-

value: 0.46, log-rank test) nor for the analysis of the baseline status alone (p-value: 0.61, log-rank test), (figure 17B).

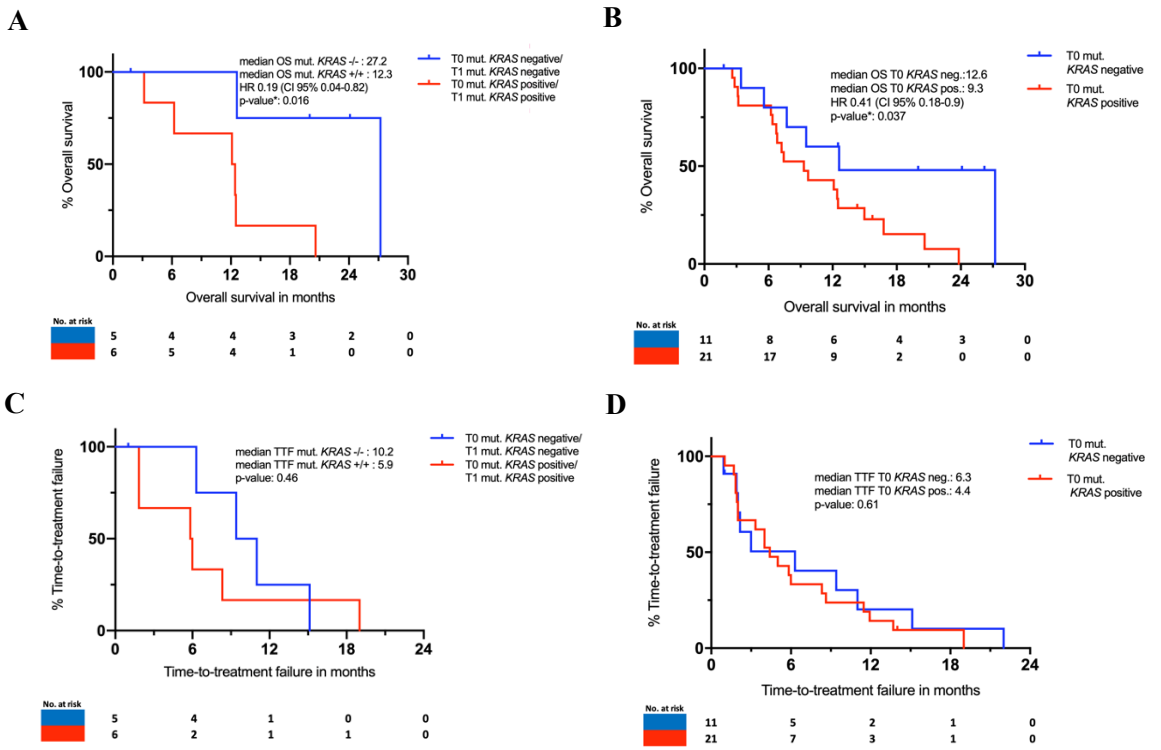

Figure 17. Survival analysis of patients with two-time point *KRAS* analysis compared to baseline *KRAS* analysis alone.

A: Median OS of the responders is 2.2 times longer than the OS of the non-responders (p-value*: 0.016, HR 0.19 CI 95% 0.04-0.82, log-rank test), (N=11). **B:** Patients without measurable mutant *KRAS* at baseline show a 1.4 times longer OS than patients with measurable mutant *KRAS* at baseline (p-value*: 0.037, HR 0.41, CI 95% 0.18-0.9, log-rank test), (N=32). **C:** Median TTF of the responders is 1.7 times longer than the TTF of the non-responders (p-value: 0.46, log-rank test), (N=11). **D:** Patients without measurable mutant *KRAS* at baseline show a 1.4 times longer TTF than patients with measurable mutant *KRAS* at baseline (p-value: 0.61, log-rank test), (N=32).

4.5 Estimation of the tissue-blood concordance

In the following, the correspondence between the detectability of mutant *KRAS* in the plasma and the mutational status of the primary tumor sample was analyzed. In 18 cases from the overall 32 patients, next-generation sequencing analysis was performed from tissue material. From these 18 cases, 17 patients had a detectable *KRAS* mutation in the tissue. To investigate how far these results

correspond with the mutational status of the plasma analysis, the tissue-blood concordance was calculated. Because only seven *KRAS* mutations are detectable by ddPCR (G12A, G12C, G12D, G12V, G12R, G12S, G13D), other *KRAS* mutations were excluded from the calculation of the tissue-blood concordance. Consequently, the tissue-blood concordance was calculated with 16 of the 17 *KRAS* mutations detected by NGS, whereas one *KRAS* mutation, a Q61H mutation, was only detectable by NGS. It was possible to detect mutant *KRAS* molecules in the blood of 11 patients out of these 16 patients. This results in a tissue-blood concordance of 68.8%. On the other hand, all of the *KRAS* mutants detected by ddPCR analysis were confirmed in the tissue sample (table 17).

To investigate whether the presence of liver metastases would influence the tissue-blood concordance, the same calculations were made when only those patients with liver metastases were considered (N=14). In this case all of the 14 patients received a tissue based NGS analysis which detected mutant *KRAS* in 100% of cases. In one of these 14 patients the above mentioned Q61H mutation was detected by NGS, which is why this patient was again excluded from the calculation of the tissue-blood concordance. In 10 of 13 cases mutant *KRAS* was also detectable in plasma, resulting in a tissue-blood concordance of 76.9% (table 18).

Table 17. Comparison between ddPCR and NGS results regarding mutant *KRAS* detection in plasma and primary tissue.

All of the *KRAS* mutations detected by ddPCR in plasma were detectable in the primary tissue. Out of 16 patients with detectable mutant *KRAS* in the primary tumor, 11 also presented detectable mutant *KRAS* in plasma.

	Time point T0 (N=32)
NGS performed	56.3% (N=18/32)
ddPCR *KRAS* positive	65.6% (N=21/32)
Tissue-blood concordance	68.8% (N=11/16)
NGS *KRAS* positive	94.4% (N=17/18)
NGS *KRAS* negative	5.6% (N=1/18)
NGS *KRAS* positive and ddPCR negative	27.8% (N=5/18)
ddPCR *KRAS* positive and NGS negative	0% (N=0/18)

Table 18. Comparison between ddPCR and NGS mutant *KRAS* detection in patients presenting liver metastases.

A *KRAS* mutation was detectable in the tumor tissue of all patients harboring liver metastases. In 10 patients the *KRAS* mutation status was confirmed by ctDNA analysis.

Time point T0 with liver metastases (N=14)	
NGS performed	100% (N=14/14)
ddPCR *KRAS* positive	71.4% (N=10/14)
Tissue-blood concordance	76.9% (N=10/13)
NGS *KRAS* positive	100% (N=14/14)
NGS *KRAS* negative	0% (N=0/14)
NGS *KRAS* positive and ddPCR negative	28.6% (N=4/14)
ddPCR *KRAS* positive and NGS negative	0% (N=0/14)

In addition to the *KRAS* analysis, the NGS assay provided an overview of the mutation status of other genes. Most frequently mutated was besides *KRAS,* the *TP53* gene in 55.6% of patients (N=10/18), followed by *SMAD4* which was mutated in 22.2% (N=4/18). In three patients a Tuberous Sclerosis 1 (*TSC1)* mutation was found (16.7%, N=3/18). Moreover, two tumor tissues contained *BRCA2* mutations (11.1%, N=2/18), another two samples a mutation of *ATM* (11.1%, N=2/18) and jet another two a mutation of *GNAS* (11.1%, N=2/18) (figure 18).

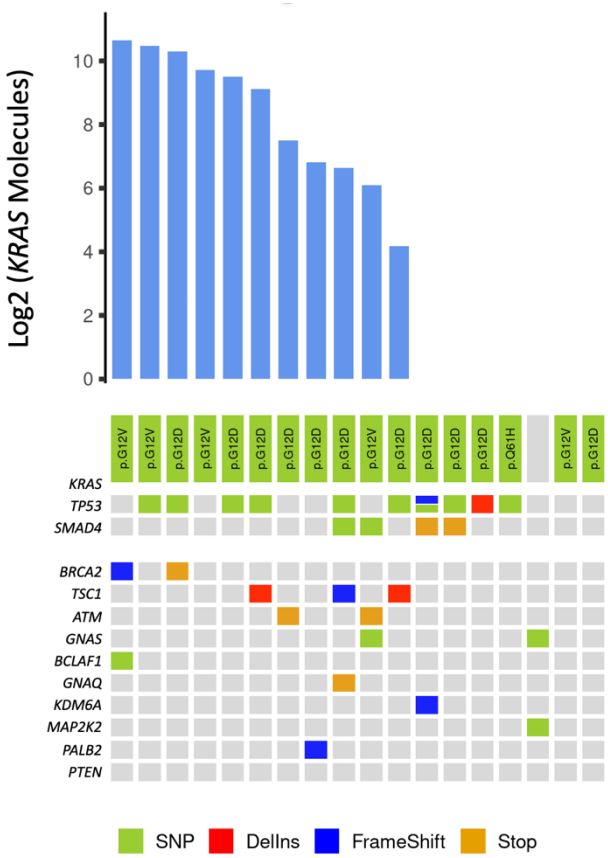

Figure 18. Oncomap presenting NGS results of the tumor tissue and the corresponding mutant *KRAS* level detected by ddPCR in plasma.

At the top, the logarithmized mutant *KRAS* level detected by ddPCR analysis of the blood are presented as bar graph. The bottom displays the respective results of the NGS gene panel for each patient. Most frequently mutated were: *KRAS* (94.4%), *TP53* (55.6%), *SMAD4* (22.2%), *TSC1* (16.7%), *BRCA2* (11.1%), *ATM* (11.1%), *GNAS* (11.1%). Detected *KRAS* mutations were divided into: G12D (61%), G12V (27.8%), Q61H (0.056%).

(This figure was made by Sven-Thorsten Liffers)

Furthermore, it was analyzed whether a mismatch in NGS and ddPCR mutation status would be reflected by a prognostic difference. The underlying idea was that the absence of ctDNA in blood, despite a confirmed *KRAS* mutation in tumor tissue, could be attributed to a less aggressive metastatic behavior of the tumor, spreading less tumor cells into the circulation.

In this matter, the OS of patients with detectable mutant *KRAS* in both the tumor tissue and in the plasma was compared to patients with just detectable mutant *KRAS* in the tissue. However, only five patients fitted to the last-named criteria and four of them were censored. This insufficient

number of patients in this category precluded a statistical comparison between the two groups but might inspire similar investigations in other studies (figure 19).

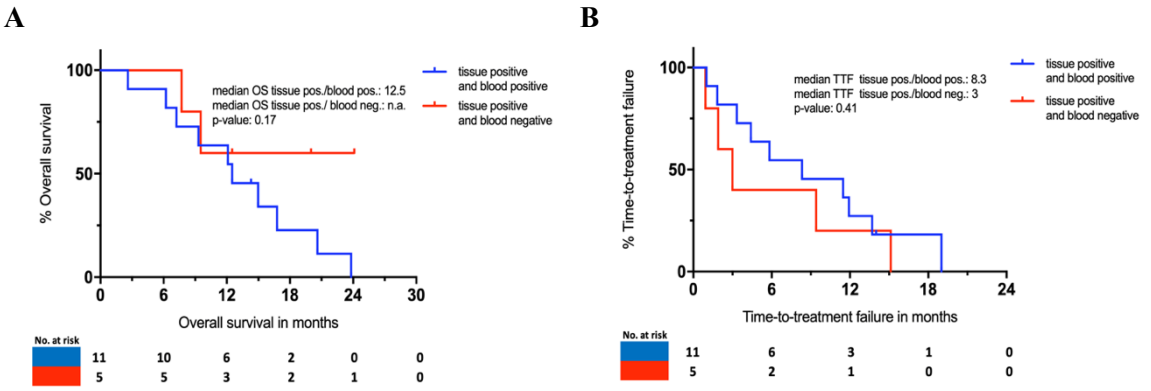

Figure 19. Kaplan-Meier curves comparing OS and TTF of patients with detectable mutant *KRAS* in both tissue and plasma to patients with a *KRAS* mutation only detectable in tumor tissue.

A: A comparison between patients with detectable mutant *KRAS* in plasma and tissue to those where *KRAS* was only detectable in the tissue was not possible (p-value: 0.17, log-rank test), (N=17). **B**: Patients with detectable mutant *KRAS* in both tissue and blood showed a longer TTF than patients who showed detectable mutant *KRAS* only in the tumor tissue (p-value: 0.41, log-rank test), (N=17).

Finally, the number of mutations in genes other than *KRAS* was compared to the respective mutant *KRAS* level in blood. If an increasing number of mutated genes in the tumor would influence the detectability of mutant *KRAS* in peripheral blood, this would decrease the ability to monitor cancer activity by mutant *KRAS* detection in blood. The NGS panel used presented a broad coverage of 47 genes. This analysis showed no significant correlation between the number of other mutations in the tissue and the mutant *KRAS* level in blood (p-value: 0.875) (Figure 20).

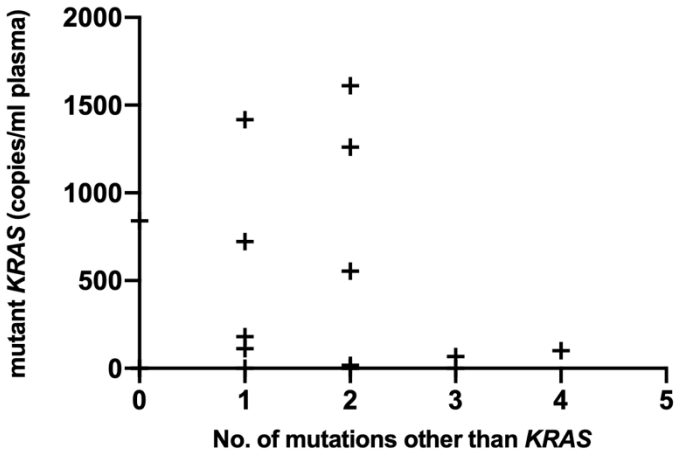

Figure 20. Impact of the mutational heterogeneity of the tumor on the mutant *KRAS* level in blood.

The number of mutations detected in the primary tumor by NGS analysis was correlated with the mutant *KRAS* level in blood. No correlation could be observed and the Spearman correlation coefficient r was -0.04 (p-value: 0.875).

5 DISCUSSION

Liquid biopsy has recently gained enormous attention in medical science and is increasingly used for biomarker characterization and clinical decision-making in various tumor entities. Especially in pancreatic cancer, where pathological and molecular diagnosis is challenging and clinical deterioration is often rapid, a simplified and robust access to molecular information of the tumor could improve treatment initiation and identification of targeted treatment options of PDAC patients. Consequently, this study aimed to explore liquid biopsy approaches in pancreatic cancer management. Therefore, the focus of this theses was a) establishment of a DNA isolation protocol for the ddPCR approach; b) explorative cfDNA analysis of pre/post treatment patient cohort; c) comparison of established means (imaging, clinical chemistry) for treatment response evaluation to ctDNA analysis regarding prognostic and predictive parameters; d) evaluation of the correspondence between mutation detection in tumor tissue and liquid biopsy samples.

5.1 Establishment of a DNA isolation protocol for the ddPCR

Optimal DNA isolation is a prerequisite for a successful ctDNA analysis. CfDNA fragments measure less than 200 bp if they derive from cancer cells, whereas germline-derived cfDNA occurs in longer fragments (Mouliere et al., 2018; Mouliere et al., 2011). Consequently, the isolation of a high proportion of small-fragmented DNA is desired to increase the amount of tumor-derived DNA for ddPCR analysis.

Therefore, three different DNA isolation kits, the Maxwell, the Qiagen and Zymo kit, were compared. The Qiagen and Zymo kits represent spin-column-based methods, whereas the Maxwell kit isolates cfDNA using magnetic beads in an automated process. The largest DNA yield of 20.6 ng/ml plasma was isolated by the Qiagen kit. This observation was confirmed by several studies, in which the Qiagen kit isolated the highest DNA yields and is consequentially frequently used in studies on ddPCR (Pérez-Barrios et al., 2016; Sorber et al., 2017).

Further analysis of the DNA fragment size isolated revealed that two kits (Zymo and Qiagen) isolated high-integrity DNA with 600 bp and smaller DNA fragments of 150-210 bp. The Maxwell kit was the only method to isolate exclusively small DNA fragments of 150-210 bp. Even though some studies have found that the Maxwell kit also isolates DNA fragments more than 200 bp, the bias of magnetic beads-based methods to isolate higher fractions of low-integrity DNA has been described previously (Bronkhorst et al., 2020; Pérez-Barrios et al., 2016; Sorber et al., 2017).

The comparability in evaluation of cfDNA isolation might be confounded due to differences in the study populations. The samples in this study originated from advanced stage lung cancer, whereas the study from Sorber et al. analyzed samples of malignant and benign pancreatic disease and Pérez-Barrios et al. investigated samples from colorectal and lung cancer patients (Pérez-Barrios et al., 2016; Sorber et al., 2017). Additionally, the sample number in this study was lower compared to other studies, which could account for differences in between the studies.

The Maxwell kit was chosen for this liquid biopsy approach because it was the only kit to exclusively isolate small-fragmented DNA. Another advantage of this kit is the fully automated process including its ability to self-sterilize after each sample prep. That enables practical feasibility of liquid biopsy especially when this method is applied for therapy monitoring, necessitating multiple sample testing in a short period. It further improves comparability in between studies because user-dependent differences are minimized, thus scientific process on liquid biopsy approaches would be facilitated.

5.2 The outcome of 5-FU- and gemcitabine-based therapy shows no difference in a real-world setting

Previous studies have proven the superiority of intensified protocols such as FOLFIRINOX and gemcitabine nab-paclitaxel towards a monotherapy with gemcitabine for palliative treatment of pancreatic cancer (Conroy et al., 2011; Von Hoff et al., 2013). However, it remains inconclusive whether patients are more likely to benefit from FOLFIRINOX or gemcitabine nab-paclitaxel (Cho et al., 2020).

Survival and treatment response analysis of a recent meta-analysis by Chiorean et al. reported median OS rates of 8.6-13.8 months for FOLFIRINOX and 6.1-14 months for gemcitabine nab-paclitaxel and a median TTF of 2.8-4.3 months for FOLFIRINOX compared to 3.4-4.3 months for gemcitabine nab-paclitaxel (Chiorean et al., 2019). Furthermore, longer survival was observed with FOLFIRINOX treatment in the majority of studies, but this difference was in most cases not significant (Chiorean et al., 2019). The survival observed in this study was within the lower range of these observations (OS 5-FU: 9.6 months, Gem-nab.: 6.4 months), whereas the median TTF ranged above previously reported data (TTF 5-FU: 5 months, Gem-nab.: 4.86 months) (Chiorean et al., 2019).

The fact that the survival rates of our study are in the lower range of literature reports, can be explained by multiple reasons. First of all, within this study no preselection of patients concerning performance status was performed to reflect a real-world treatment setting. Unlike large prospective studies that typically exclude patients with an ECOG status above 1 (Conroy et al., 2018; Von Hoff et al., 2013), 14.3% of the patients in this study had an ECOG status higher than one.

Moreover, only 75% of the administered gemcitabine-based treatments consisted of intensified protocols with gemcitabine-nab-paclitaxel and 90% of the 5-FU-based treatments represented intensified protocols with FOLFIRINOX. In the remaining 25% of gemcitabine-based treatments and 10% of 5-FU-based treatments, gemcitabine mono therapy or FOLFOX was administered, respectively. This could explain lower survival rates compared to studies in which 100% of patients received intensified protocols (Cho et al., 2020; Kang et al., 2018). Furthermore, this study observed a slightly increased median survival in favor of 5-FU-based protocols which was, in agreement with the meta-analysis from Chiorean et al., not significant (median OS 5-FU-based: 9.6 months vs OS gemcitabine-based: 6.4 months) (figure 8A) (Chiorean et al., 2019).

Another influence on the treatment outcome might be the increased age of the patients that received gemcitabine-based treatment, compared to patients with 5-FU-based 1st line (55 years vs 65.6 years, p-value*: 0.007, log-rank test). This difference has also been reported by previous studies that described a tendency to administer gemcitabine-based therapy to older patients with worse

ECOG status (Chiorean et al., 2019; Cho et al., 2020). A reason for this could be that adverse events are known to occur more frequently with 5-FU-based therapy regimen, including febrile neutropenia, diarrhea and nausea and are therefore administered to patients in reduced condition reluctantly (Chiorean et al., 2019; Conroy et al., 2011; Conroy et al., 2018; Pusceddu et al., 2019). Concluding from that, 5-FU- and gemcitabine-based protocols were compared in a real-world setting with no clear tendency favoring one regimen based upon response and survival (Chiorean et al., 2019; S. Kim et al., 2018).

5.3 Comparison of mutant *KRAS* detection rates with literature

In this work, a *KRAS* mutation was detectable in 65.6% of patient samples with a median MAF of 6.15%, which was within the range of previous studies where mutant *KRAS* was detected in 38.2-77.9% of cases with a median MAF ranging from 2.8 to 94% (Bernard et al., 2019; Creemers et al., 2017; Hadano et al., 2016; M. K. Kim et al., 2018; Mohan et al., 2019; Strijker et al., 2020; Sugimori et al., 2020; Toledano-Fonseca et al., 2020).

Notably, DNA concentrations documented in other studies ranged from 33 to 427 ng/ml plasma, which is higher than the median DNA concentration of 15.5 ng/ml plasma in this study (S. Kim et al., 2018; Strijker et al., 2020; Toledano-Fonseca et al., 2020). These studies used the Qiagen kit, which isolates higher overall DNA yield as shown in the result section (table 4), perhaps explaining the difference in DNA concentrations.

Mutant *KRAS* detection rates and MAF observed in this work were comparable with other studies despite the lower total cfDNA yield per sample, thus rendering the Maxwell kit is suitable for cfDNA isolation.

5.4 Mutant *KRAS* has the potential to improve prognostic patient stratification

The comparison between the prognostic value of CA 19-9 and mutant *KRAS* status showed a significant correlation with reduced OS for both biomarkers (CA 19-9 p-value*: 0.024, mutant *KRAS* p-value*: 0.037, log-rank test), whereas only elevated CA 19-9 correlated significantly with reduced median TTF (CA 19-9 p-value*: 0.018, mutant *KRAS* p-value: 0.604, log-rank test).

A comparison between these two biomarkers has been frequently discussed in literature and the data on this topic show no trend which favors one marker over the other. Some studies also found a significant association between CA 19-9 and worse OS and PFS, supporting the findings of this study (Bernard et al., 2019; Toledano-Fonseca et al., 2020). Other studies found no correlation between CA 19-9 level and survival in contrast to their ctDNA analysis, concluding superiority of mutant *KRAS* detection as biomarker (Strijker et al., 2020; Watanabe et al., 2019).

The fact that 6% of Caucasian people and 22% of the African American population are not able to produce CA 19-9 at all highly restricts the usability of CA 19-9 as a biomarker (Tempero et al., 1987). Further, in patients with obstructive jaundice, which frequently occurs within the primary diagnosis of pancreatic cancer, CA 19-9 level showed no correlation with progressive disease (Bernard et al., 2019).

The simple subdivision of CA 19-9 using the upper limit of normal (37 U/ml) has neither in this analysis nor in many other studies a prognostic or predictive information.

Various cut-off values for CA 19-9 have been determined between studies, with which a significant prognostic stratification could be observed. However, no cut-off value for CA 19-9 was described that could prove a reproducible prognostic value in independent studies (Ballehaninna & Chamberlain, 2012; Watanabe et al., 2019).

In this matter, mutant *KRAS* detection presents an advantage. The simple distribution between detectable and undetectable mutant *KRAS* in many independent studies held prognostic significance (S. Kim et al., 2018; Pietrasz et al., 2017; Strijker et al., 2020; Watanabe et al., 2019). In contrast to this analysis, other studies were able to show a significant association of mutant *KRAS* detectability and median PFS as well (Bernard et al., 2019; Toledano-Fonseca et al., 2020). However, this exploratory retrospective study was not powered to address this question.

This work supports the hypothesis that the detectability of mutant *KRAS* itself correlates with the prognosis and has therefore potential to aid prognostic stratification of PDAC patients. These observations should encourage for further evaluation of liquid biopsy in prospective well-powered clinical trials.

5.5 MAF improves the prognostic value of mutant *KRAS* detection

As previously reported, the mutant allele fraction (MAF) has been reported to have a better prognostic value than the *KRAS* status in plasma alone (Bernard et al., 2019; Sugimori et al., 2020; Toledano-Fonseca et al., 2020). This work investigated whether these findings also apply to this liquid biopsy approach and found that reduced overall survival could be observed when the baseline MAF exceeded 1.5% (figure 12D). As compared to the baseline mutant *KRAS* assessment alone or to the subdivision of mutant *KRAS* in high and low copy-numbers, there was a greater difference in survival. Therefore, these data support the observation of previous studies on the prognostic value of the MAF. Notably, similar to the previous mentioned problem with a cut-off for CA 19-9, there is currently no consensus on the ideal cut-off for the MAF, hence further research on this topic is needed to investigate this biomarker.

5.6 Treatment monitoring by mutant *KRAS* is feasible

An adequate therapeutic monitoring and early detection of progression are crucial not only for individual treatment decision, but also for the evaluation of new treatment regimens in clinical trials. However, the established methods for treatment monitoring, which are CA 19-9 measurement and CT-imaging, have known pitfalls in measuring treatment response.

Apart from the previous mentioned limitations of CA 19-9, there are also issues concerning CT imaging for response monitoring. The measurement of tumor borders in CT images is challenging especially for primary pancreatic cancer because this tumor is morphologically difficult to differentiate from surrounding tissue due to its high stromal content (Tjensvoll et al., 2016). As a consequence, CT analysis is often imprecise in reflecting therapeutic efficacy, hence liquid biopsy could improve diagnostics when CT findings remain inconclusive (Strijker et al., 2020).

Previous studies support the hypothesis that ctDNA analysis does indeed enable early detection of tumor progress (Sugimori et al., 2020; Toledano-Fonseca et al., 2020; Watanabe et al., 2019). As an example, a study by Sausen et al. found that ctDNA increase following resection detected

recurrence after an average of 3.1 months, whereas CT-imaging took an average of 9.6 months to detect disease progression (Sausen et al., 2015).

In the context of this work, the explorative analysis of six patients with longitudinal sampling time points observed detectable mutant *KRAS* in plasma of all patients before treatment onset. Shortly after 1st line treatment was administered, mutant *KRAS* levels decreased below the limit of detection, indicating a treatment response. In half of the examples (patient 11, patient 13, patient 5) mutant *KRAS* levels were elevated 8-50 days before progressive disease was radiologically confirmed. Interestingly, in these three patients the CT image documented a partial regression or stable disease during the same time period as mutant *KRAS* level increased. Additionally, another two patients showed a rise of mutant *KRAS* values simultaneously (patient 64) and shortly after (patient 2) radiological confirmation of disease progression.

One patient (patient 68) presented decreasing mutant *KRAS* level at a time point where rising CA 19-9 level and CT-imaging both indicated a progression. A possible explanation for this observation would be that a mutation other than *KRAS* played a leading role in the progression of this tumor, which remains to be analyzed.

The interpretation of these results is limited by the retrospective character of the analysis, the small patient sample size and variable sampling intervals. It remains uncertain if the CT would have already detected tumor growth at the time point of elevating mutant *KRAS* level. Further, in cases where the rise of mutant *KRAS* level was detected simultaneously or subsequent to CT imaging, it is not clear whether more frequent sampling would have detected a rise of mutant *KRAS* values earlier.

In general, this analysis suggests that treatment monitoring by mutant *KRAS* detection is feasible but further prospective studies with a larger cohort, standardized and frequent sampling time points are essential to draw significant conclusions.

5.7 The therapy-naive sampling time point shows better prognostic value than the follow-up assessment

Within this study, the baseline *KRAS* status was compared to the *KRAS* status up to 50 days after start of therapy, to examine which one predicted the prognosis better.

When comparing the relevance of a baseline ctDNA assessment to the follow-up analysis, several studies had inconclusive results. Some reported an even stronger prognostic value of measurable mutant *KRAS* at follow-up time points, compared to the baseline value (Del Re et al., 2017; Tjensvoll et al., 2016; Watanabe et al., 2019). Others reported a stronger value of the therapy-naive sampling time point, which was significantly associated with OS and PFS (Hadano et al., 2016; Toledano-Fonseca et al., 2020).

Our work suggests that the individual analysis of mutant *KRAS* after start of therapy is less expressive, compared to the therapy-naive mutant *KRAS* status and correlates neither with OS nor TTF significantly. Nevertheless, absence of mutant *KRAS* before and after start of therapy presented a slightly better correlation with increased OS than the baseline mutant *KRAS* status alone. However, again a major limitation is the low sample size, thus, these observations are exploratory and necessitate well-controlled clinical trials for further assessment.

5.8 Liquid Biopsy has the potential to determine mutant *KRAS* status in metastatic patients

The current gold standard to identify the mutation pattern of the individual tumor is the tissue analysis, nowadays typically by next-generation sequencing (NGS).

Not seldomly, low tumor cellularity limits reliable mutation calling from the tumor tissue (Buscail et al., 2019). Especially in pancreatic cancer, in which a high stromal content and low tumor cellularity is highly frequent, this remains an important disadvantage of a tissue biopsy-based approach (Buscail et al., 2019; Chang et al., 1997). For metastatic disease, where tumor resection is not indicated, the risks of an invasive biopsy for molecular analysis should be considered with care. In those cases where initial biopsy did not provide sufficient material for molecular analysis, a liquid biopsy could prevent the risks that a frequent repetition of invasive biopsy bears.

Therefore, this work aimed to explore the reliability with which the mutation status of *KRAS* was reflected by liquid biopsy analysis. For this purpose, matching tissue samples were analyzed using NGS and the concordance between both procedures was calculated as tissue-blood concordance.

The tissue-blood concordance in this study was 68.8%, which means that in this percent of cases, a *KRAS* mutation detected by NGS analysis in the tissue sample (gold standard) was also detectable in the respective ctDNA sample at baseline. This result lays within the data range of other studies that detected a tissue-blood concordance of 51-90% (Bernard et al., 2019; M. K. Kim et al., 2018; Sugimori et al., 2020; Toledano-Fonseca et al., 2020; Watanabe et al., 2019).

A major difficulty of the cfDNA analysis lays within the extremely low DNA yield, which could explain the discrepancy between mutational status in the tissue and the liquid biopsy (Mohan et al., 2019; Mouliere et al., 2018).

Further, a positive correlation between cfDNA yield, tumor stage and tumor mass has been described previously (Dawson et al., 2013; Schwarzenbach et al., 2012). This would explain why a study from Garcia et al. documented higher tissue-blood concordance among patients with metastatic colorectal cancer, compared to those with localized disease (Garcia et al., 2018).

Accordingly, our work reported higher ctDNA detection rates and a higher tissue-blood concordance when only patients with liver metastases were considered.

In summary, the detection of mutant *KRAS* is consistent with the tissue *KRAS* status in the majority of cases and the concordance increases with tumor stage, presence of metastases and higher tumor load. This underpins that especially for metastatic PDAC, where tissue biopsy is typically not performed from tumor resection, liquid biopsy has the potential to determine the mutation status of *KRAS* and, in the future, likely of other cancer genes alterations such as *BRCA*1/2, microsatellite instability or tumor mutational burden and thus could add to the diagnostic workup.

6 SUMMARY

This work aimed to contribute to the evaluation of a liquid biopsy approach in pancreatic cancer management and explored this method for prognostic patient stratification as well as treatment monitoring and tumor response evaluation. For this purpose, a suitable cell-free DNA (cfDNA) isolation method was identified and then digital droplet Polymerase chain reaction (ddPCR) mutant Kirsten Rat Sarcoma Gene (*KRAS)* detection was performed on advanced pancreatic ductal adenocarcinoma (PDAC) patient samples before and during chemotherapeutic treatment.

In contrast to two other DNA isolation kits, the Maxwell cfDNA isolation kit was found to be most suitable for circulating tumor DNA (ctDNA) isolation because it isolates exclusively small-fragmented DNA. Using this DNA isolation method, liquid biopsy assessment was feasible and in the majority of patients the *KRAS* mutations detectable in tumor tissue could also be confirmed in the plasma.

Moreover, without a cut-off value needed, the absence of mutant *KRAS* in plasma was associated with a better overall survival and this relation increased when mutant *KRAS* remained untraceable after treatment onset.

Finally, the explorative analysis of treatment monitoring by liquid biopsy was promising and in the majority of cases, albeit at limited case numbers, the *KRAS* dynamics mirrored the clinical course of the disease and detected tumor progress simultaneously or even earlier than the computed tomography (CT).

These findings emphasize the enormous potential of ctDNA mutant *KRAS* detection as a non-invasive tool for prognostic stratification and therapy monitoring in PDAC and should inspire and assist the design of further studies on this topic.

7 LITERATURE

1. Agarwal, B., Abu-Hamda, E., Molke, K. L., Correa, A. M.,Ho, L. (2004): Endoscopic ultrasound-guided fine needle aspiration and multidetector spiral CT in the diagnosis of pancreatic cancer. Am J Gastroenterol 99, 844-850.

2. Aguirre, A. J., Nowak, J. A., Camarda, N. D., Moffitt, R. A., Ghazani, A. A., Hazar-Rethinam, M., Raghavan, S., Kim, J., Brais, L. K., Ragon, D., Welch, M. W., Reilly, E., McCabe, D., Marini, L., Anderka, K., Helvie, K., Oliver, N., Babic, A., Da Silva, A., Nadres, B., Van Seventer, E. E., Shahzade, H. A., St Pierre, J. P., Burke, K. P., Clancy, T., Cleary, J. M., Doyle, L. A., Jajoo, K., McCleary, N. J., Meyerhardt, J. A., Murphy, J. E., Ng, K., Patel, A. K., Perez, K., Rosenthal, M. H., Rubinson, D. A., Ryou, M., Shapiro, G. I., Sicinska, E., Silverman, S. G., Nagy, R. J., Lanman, R. B., Knoerzer, D., Welsch, D. J., Yurgelun, M. B., Fuchs, C. S., Garraway, L. A., Getz, G., Hornick, J. L., Johnson, B. E., Kulke, M. H., Mayer, R. J., Miller, J. W., Shyn, P. B., Tuveson, D. A., Wagle, N., Yeh, J. J., Hahn, W. C., Corcoran, R. B., Carter, S. L.,Wolpin, B. M. (2018): Real-time Genomic Characterization of Advanced Pancreatic Cancer to Enable Precision Medicine. Cancer discovery 8, 1096-1111.

3. Al-Hawary, M. M., Francis, I. R., Chari, S. T., Fishman, E. K., Hough, D. M., Lu, D. S., Macari, M., Megibow, A. J., Miller, F. H., Mortele, K. J., Merchant, N. B., Minter, R. M., Tamm, E. P., Sahani, D. V.,Simeone, D. M. (2014): Pancreatic ductal adenocarcinoma radiology reporting template: consensus statement of the Society of Abdominal Radiology and the American Pancreatic Association. Radiology 270, 248-260.

4. Apte, M. V., Park, S., Phillips, P. A., Santucci, N., Goldstein, D., Kumar, R. K., Ramm, G. A., Buchler, M., Friess, H., McCarroll, J. A., Keogh, G., Merrett, N., Pirola, R.,Wilson, J. S. (2004): Desmoplastic reaction in pancreatic cancer: role of pancreatic stellate cells. Pancreas 29, 179-187.

5. Bailey, P., Chang, D. K., Nones, K., Johns, A. L., Patch, A. M., Gingras, M. C., Miller, D. K., Christ, A. N., Bruxner, T. J., Quinn, M. C., Nourse, C., Murtaugh, L. C., Harliwong, I., Idrisoglu, S., Manning, S., Nourbakhsh, E., Wani, S., Fink, L., Holmes, O., Chin, V., Anderson, M. J., Kazakoff, S., Leonard, C., Newell, F., Waddell, N., Wood, S., Xu, Q., Wilson, P. J., Cloonan, N., Kassahn, K. S., Taylor, D., Quek, K., Robertson, A., Pantano, L., Mincarelli, L., Sanchez, L. N., Evers, L., Wu, J., Pinese, M., Cowley, M. J., Jones, M. D., Colvin, E. K., Nagrial, A. M., Humphrey, E. S., Chantrill, L. A., Mawson, A., Humphris, J., Chou, A., Pajic, M., Scarlett, C. J., Pinho, A. V., Giry-Laterriere, M., Rooman, I., Samra, J. S., Kench, J. G., Lovell, J. A., Merrett, N. D., Toon, C. W., Epari, K., Nguyen, N. Q., Barbour, A., Zeps, N., Moran-Jones, K., Jamieson, N. B., Graham, J. S., Duthie, F., Oien, K., Hair, J., Grutzmann, R., Maitra, A., Iacobuzio-Donahue, C. A., Wolfgang, C. L., Morgan, R. A., Lawlor, R. T., Corbo, V., Bassi, C., Rusev, B., Capelli, P., Salvia, R., Tortora, G., Mukhopadhyay, D., Petersen, G. M., Munzy, D. M., Fisher, W. E., Karim, S. A., Eshleman, J. R., Hruban, R. H., Pilarsky, C., Morton, J. P., Sansom, O. J., Scarpa, A., Musgrove, E. A., Bailey, U. M., Hofmann, O., Sutherland, R. L., Wheeler, D. A., Gill, A. J., Gibbs, R. A., Pearson, J. V., Waddell, N., Biankin, A. V.,Grimmond, S. M. (2016): Genomic analyses identify molecular subtypes of pancreatic cancer. Nature 531, 47-52.

6. Ballehaninna, U. K.,Chamberlain, R. S. (2012): The clinical utility of serum CA 19-9 in the diagnosis, prognosis and management of pancreatic adenocarcinoma: An evidence based appraisal. J Gastrointest Oncol 3, 105-119.

7. Bernard, V., Kim, D. U., San Lucas, F. A., Castillo, J., Allenson, K., Mulu, F. C., Stephens, B. M., Huang, J., Semaan, A., Guerrero, P. A., Kamyabi, N., Zhao, J., Hurd, M. W., Koay, E. J., Taniguchi, C. M., Herman, J. M., Javle, M., Wolff, R., Katz, M., Varadhachary, G., Maitra, A.,Alvarez, H. A. (2019): Circulating Nucleic Acids Are Associated With Outcomes of Patients With Pancreatic Cancer. Gastroenterology 156, 108-118.e104.

8. Birkmeyer, J. D., Siewers, A. E., Finlayson, E. V. A., Stukel, T. A., Lucas, F. L., Batista, I., Welch, H. G.,Wennberg, D. E. (2002): Hospital Volume and Surgical Mortality in the United States. New England Journal of Medicine 346, 1128-1137.

9. Blakely, C. M., Watkins, T. B. K., Wu, W., Gini, B., Chabon, J. J., McCoach, C. E., McGranahan, N., Wilson, G. A., Birkbak, N. J., Olivas, V. R., Rotow, J., Maynard, A., Wang, V., Gubens, M. A., Banks, K. C., Lanman, R. B., Caulin, A. F., St John, J., Cordero, A. R., Giannikopoulos, P., Simmons, A. D., Mack, P. C., Gandara, D. R., Husain, H., Doebele, R. C., Riess, J. W., Diehn, M., Swanton, C.,Bivona, T. G. (2017): Evolution and clinical impact of co-occurring genetic alterations in advanced-stage EGFR-mutant lung cancers. Nature Genetics 49, 1693-1704.

10. Bosman, F. T., Carneiro, F., Hruban, R. H.,Theise, N. D. (2010): WHO classification of tumours of the digestive system: World Health Organization.

11. Bournet, B., Muscari, F., Buscail, C., Assenat, E., Barthet, M., Hammel, P., Selves, J., Guimbaud, R., Cordelier, P.,Buscail, L. (2016): KRAS G12D Mutation Subtype Is A Prognostic Factor for Advanced Pancreatic Adenocarcinoma. Clin Transl Gastroenterol 7, e157.

12. Bronkhorst, A. J., Ungerer, V.,Holdenrieder, S. (2020): Comparison of methods for the isolation of cell-free DNA from cell culture supernatant. Tumor Biology 42, 1010428320916314.

13. Brychta, N., Krahn, T.,von Ahsen, O. (2016): Detection of KRAS Mutations in Circulating Tumor DNA by Digital PCR in Early Stages of Pancreatic Cancer. Clinical Chemistry 62, 1482-1491.

14. Buscail, E., Maulat, C., Muscari, F., Chiche, L., Cordelier, P., Dabernat, S., Alix-Panabieres, C.,Buscail, L. (2019): Liquid Biopsy Approach for Pancreatic Ductal Adenocarcinoma. Cancers (Basel) 11

15. Cameron, J. L., Riall, T. S., Coleman, J.,Belcher, K. A. (2006): One thousand consecutive pancreaticoduodenectomies. Annals of surgery 244, 10-15.

16. Cascinu, S., Falconi, M., Valentini, V., Jelic, S.,Group, E. G. W. (2010): Pancreatic cancer: ESMO Clinical Practice Guidelines for diagnosis, treatment and follow-up. Annals of oncology : official journal of the European Society for Medical Oncology 21 Suppl 5, v55-58.

17. Chang, K. J., Nguyen, P., Erickson, R. A., Durbin, T. E.,Katz, K. D. (1997): The clinical utility of endoscopic ultrasound-guided fine-needle aspiration in the diagnosis and staging of pancreatic carcinoma. Gastrointest Endosc 45, 387-393.

18. Chiorean, E. G., Cheung, W. Y., Giordano, G., Kim, G.,Al-Batran, S.-E. (2019): Real-world comparative effectiveness of nab-paclitaxel plus gemcitabine versus FOLFIRINOX in advanced pancreatic cancer: a systematic review. Therapeutic advances in medical oncology 11, 1758835919850367-1758835919850367.

19. Cho, I. R., Kang, H., Jo, J. H., Lee, H. S., Chung, M. J., Park, J. Y., Park, S. W., Song, S. Y., An, C., Park, M.-S.,Bang, S. (2020): FOLFIRINOX vs gemcitabine/nab-paclitaxel for treatment of metastatic pancreatic cancer: Single-center cohort study. World journal of gastrointestinal oncology 12, 182-194.

20. Collins, M. A., Bednar, F., Zhang, Y., Brisset, J.-C., Galbán, S., Galbán, C. J., Rakshit, S., Flannagan, K. S., Adsay, N. V.,Pasca di Magliano, M. (2012a): Oncogenic Kras is required for both the initiation and maintenance of pancreatic cancer in mice. The Journal of Clinical Investigation 122, 639-653.

21. Collins, M. A., Brisset, J.-C., Zhang, Y., Bednar, F., Pierre, J., Heist, K. A., Galbán, C. J., Galbán, S.,di Magliano, M. P. (2012b): Metastatic pancreatic cancer is dependent on oncogenic Kras in mice. PloS one 7, e49707-e49707.

22. Cong, L., Liu, Q., Zhang, R., Cui, M., Zhang, X., Gao, X., Guo, J., Dai, M., Zhang, T., Liao, Q.,Zhao, Y. (2018): Tumor size classification of the 8th edition of TNM staging system is superior to that of the 7th edition in predicting the survival outcome of pancreatic cancer patients after radical resection and adjuvant chemotherapy. Scientific Reports 8, 10383.

23. Conroy, T., Desseigne, F., Ychou, M., Bouché, O., Guimbaud, R., Bécouarn, Y., Adenis, A., Raoul, J.-L., Gourgou-Bourgade, S., de la Fouchardière, C., Bennouna, J., Bachet, J.-B., Khemissa-Akouz, F., Péré-Vergé, D., Delbaldo, C., Assenat, E., Chauffert, B., Michel, P., Montoto-Grillot, C.,Ducreux, M. (2011): FOLFIRINOX versus Gemcitabine for Metastatic Pancreatic Cancer. New England Journal of Medicine 364, 1817-1825.

24. Conroy, T., Hammel, P., Hebbar, M., Ben Abdelghani, M., Wei, A. C., Raoul, J.-L., Choné, L., Francois, E., Artru, P., Biagi, J. J., Lecomte, T., Assenat, E., Faroux, R., Ychou, M., Volet, J., Sauvanet, A., Breysacher, G., Di Fiore, F., Cripps, C., Kavan, P., Texereau, P., Bouhier-Leporrier, K., Khemissa-Akouz, F., Legoux, J.-L., Juzyna, B., Gourgou, S., O'Callaghan, C. J., Jouffroy-Zeller, C., Rat, P., Malka, D., Castan, F.,Bachet, J.-B. (2018): FOLFIRINOX or Gemcitabine as Adjuvant Therapy for Pancreatic Cancer. New England Journal of Medicine 379, 2395-2406.

25. Corcoran, R. B.,Chabner, B. A. (2018): Application of Cell-free DNA Analysis to Cancer Treatment. New England Journal of Medicine 379, 1754-1765.

26. Creemers, A., Krausz, S., Strijker, M., van der Wel, M. J., Soer, E. C., Reinten, R. J., Besselink, M. G., Wilmink, J. W., van de Vijver, M. J., van Noesel, C. J. M., Verheij, J., Meijer, S. L., Dijk, F., Bijlsma, M. F., van Oijen, M. G. H.,van Laarhoven, H. W. M. (2017): Clinical value of ctDNA in upper-GI cancers: A systematic review and meta-analysis. Biochimica et Biophysica Acta (BBA) - Reviews on Cancer 1868, 394-403.

27. Crowley, E., Di Nicolantonio, F., Loupakis, F.,Bardelli, A. (2013): Liquid biopsy: monitoring cancer-genetics in the blood. Nature Reviews Clinical Oncology 10, 472-484.

28. Dawson, S. J., Tsui, D. W., Murtaza, M., Biggs, H., Rueda, O. M., Chin, S. F., Dunning, M. J., Gale, D., Forshew, T., Mahler-Araujo, B., Rajan, S., Humphray, S., Becq, J., Halsall, D., Wallis, M., Bentley, D., Caldas, C.,Rosenfeld, N. (2013): Analysis of circulating tumor DNA to monitor metastatic breast cancer. N Engl J Med 368, 1199-1209.

29. Del Re, M., Vivaldi, C., Rofi, E., Vasile, E., Miccoli, M., Caparello, C., d'Arienzo, P. D., Fornaro, L., Falcone, A.,Danesi, R. (2017): Early changes in plasma DNA levels of mutant KRAS as a sensitive marker of response to chemotherapy in pancreatic cancer. Scientific reports 7, 7931-7931.

30. di Magliano, M. P.,Logsdon, C. D. (2013): Roles for KRAS in pancreatic tumor development and progression. Gastroenterology 144, 1220-1229.

31. Diehl, F., Li, M., Dressman, D., He, Y., Shen, D., Szabo, S., Diaz, L. A., Jr., Goodman, S. N., David, K. A., Juhl, H., Kinzler, K. W.,Vogelstein, B. (2005): Detection and quantification of mutations in the plasma of patients with colorectal tumors. Proc Natl Acad Sci U S A 102, 16368-16373.

32. Diehl, F., Schmidt, K., Choti, M. A., Romans, K., Goodman, S., Li, M., Thornton, K., Agrawal, N., Sokoll, L., Szabo, S. A., Kinzler, K. W., Vogelstein, B.,Diaz, L. A., Jr. (2008): Circulating mutant DNA to assess tumor dynamics. Nat Med 14, 985-990.

33. Ducreux, M., Cuhna, A. S., Caramella, C., Hollebecque, A., Burtin, P., Goere, D., Seufferlein, T., Haustermans, K., Van Laethem, J. L., Conroy, T.,Arnold, D. (2015): Cancer of the pancreas: ESMO Clinical Practice Guidelines for diagnosis, treatment and follow-up. Ann Oncol 26 Suppl 5, v56-68.

34. Eisenhauer, E. A., Therasse, P., Bogaerts, J., Schwartz, L. H., Sargent, D., Ford, R., Dancey, J., Arbuck, S., Gwyther, S., Mooney, M., Rubinstein, L., Shankar, L., Dodd, L., Kaplan, R., Lacombe, D.,Verweij, J. (2009): New response evaluation criteria in solid tumours: revised RECIST guideline (version 1.1). Eur J Cancer 45, 228-247.

35. Ene-Obong, A., Clear, A. J., Watt, J., Wang, J., Fatah, R., Riches, J. C., Marshall, J. F., Chin-Aleong, J., Chelala, C., Gribben, J. G., Ramsay, A. G.,Kocher, H. M. (2013): Activated pancreatic stellate cells sequester CD8+ T cells to reduce their infiltration of the juxtatumoral compartment of pancreatic ductal adenocarcinoma. Gastroenterology 145, 1121-1132.

36. Forbes, S. A., Bindal, N., Bamford, S., Cole, C., Kok, C. Y., Beare, D., Jia, M., Shepherd, R., Leung, K., Menzies, A., Teague, J. W., Campbell, P. J., Stratton, M. R.,Futreal, P. A. (2011): COSMIC: mining complete cancer genomes in the Catalogue of Somatic Mutations in Cancer. Nucleic Acids Res 39, D945-950.

37. Garcia, J., Forestier, J., Dusserre, E., Wozny, A.-S., Geiguer, F., Merle, P., Tissot, C., Ferraro-Peyret, C., Jones, F. S., Edelstein, D. L., Cheynet, V., Bardel, C., Vilchez, G., Xu, Z., Bringuier, P. P., Barritault, M., Brengle-Pesce, K., Guillet, M., Chauvenet, M., Manship, B., Brevet, M., Rodriguez-Lafrasse, C., Hervieu, V., Couraud, S., Walter, T.,Payen, L. (2018): Cross-platform comparison for the detection of RAS mutations in cfDNA (ddPCR Biorad detection assay, BEAMing assay, and NGS strategy). Oncotarget 9, 21122-21131.

38. Giard, D. J., Aaronson, S. A., Todaro, G. J., Arnstein, P., Kersey, J. H., Dosik, H.,Parks, W. P. (1973): In Vitro Cultivation of Human Tumors: Establishment of Cell Lines Derived From a Series of Solid Tumors2. JNCI: Journal of the National Cancer Institute 51, 1417-1423.

39. Golan, T., Hammel, P., Reni, M., Van Cutsem, E., Macarulla, T., Hall, M. J., Park, J.-O., Hochhauser, D., Arnold, D., Oh, D.-Y., Reinacher-Schick, A., Tortora, G., Algül, H., O'Reilly, E. M., McGuinness, D., Cui, K. Y., Schlienger, K., Locker, G. Y.,Kindler, H. L. (2019): Maintenance Olaparib for Germline BRCA-Mutated Metastatic Pancreatic Cancer. The New England journal of medicine 381, 317-327.

40. Goyal, L., Saha, S. K., Liu, L. Y., Siravegna, G., Leshchiner, I., Ahronian, L. G., Lennerz, J. K., Vu, P., Deshpande, V., Kambadakone, A., Mussolin, B., Reyes, S., Henderson, L., Sun, J. E., Van Seventer, E. E., Gurski, J. M., Baltschukat, S., Schacher-Engstler, B., Barys, L., Stamm, C., Furet, P., Ryan, D. P., Stone, J. R., Iafrate, A. J., Getz, G., Porta, D. G., Tiedt, R., Bardelli, A., Juric, D., Corcoran, R. B., Bardeesy, N.,Zhu, A. X. (2017): Polyclonal Secondary FGFR2 Mutations Drive Acquired Resistance to FGFR Inhibition in Patients with FGFR2 Fusion–Positive Cholangiocarcinoma. Cancer Discovery 7, 252-263.

41. Hadano, N., Murakami, Y., Uemura, K., Hashimoto, Y., Kondo, N., Nakagawa, N., Sueda, T.,Hiyama, E. (2016): Prognostic value of circulating tumour DNA in patients undergoing curative resection for pancreatic cancer. Br J Cancer 115, 59-65.

42. Hamana, K., Uzawa, K., Ogawara, K., Shiiba, M., Bukawa, H., Yokoe, H.,Tanzawa, H. (2005): Monitoring of circulating tumour-associated DNA as a prognostic tool for oral squamous cell carcinoma. Br J Cancer 92, 2181-2184.

43. Hu, Z. I., Shia, J., Stadler, Z. K., Varghese, A. M., Capanu, M., Salo-Mullen, E., Lowery, M. A., Diaz, L. A., Jr., Mandelker, D., Yu, K. H., Zervoudakis, A., Kelsen, D. P., Iacobuzio-Donahue, C. A., Klimstra, D. S., Saltz, L. B., Sahin, I. H.,O'Reilly, E. M. (2018): Evaluating Mismatch Repair Deficiency in Pancreatic Adenocarcinoma: Challenges and Recommendations. Clin Cancer Res 24, 1326-1336.

44. Jahr, S., Hentze, H., Englisch, S., Hardt, D., Fackelmayer, F. O., Hesch, R.-D.,Knippers, R. (2001): DNA Fragments in the Blood Plasma of Cancer Patients: Quantitations and Evidence for Their Origin from Apoptotic and Necrotic Cells. Cancer Research 61, 1659-1665.

45. Janes, M. R., Zhang, J., Li, L. S., Hansen, R., Peters, U., Guo, X., Chen, Y., Babbar, A., Firdaus, S. J., Darjania, L., Feng, J., Chen, J. H., Li, S., Li, S., Long, Y. O., Thach, C., Liu, Y., Zarieh, A., Ely, T., Kucharski, J. M., Kessler, L. V., Wu, T., Yu, K., Wang, Y., Yao, Y., Deng, X., Zarrinkar, P. P., Brehmer, D., Dhanak, D., Lorenzi, M. V., Hu-Lowe, D., Patricelli, M. P., Ren, P.,Liu, Y. (2018): Targeting KRAS Mutant Cancers with a Covalent G12C-Specific Inhibitor. Cell 172, 578-589.e517.

46. Jones, S., Zhang, X., Parsons, D. W., Lin, J. C., Leary, R. J., Angenendt, P., Mankoo, P., Carter, H., Kamiyama, H., Jimeno, A., Hong, S. M., Fu, B., Lin, M. T., Calhoun, E. S., Kamiyama, M., Walter, K., Nikolskaya, T., Nikolsky, Y., Hartigan, J., Smith, D. R., Hidalgo, M., Leach, S. D., Klein, A. P., Jaffee, E. M., Goggins, M., Maitra, A., Iacobuzio-Donahue, C., Eshleman, J. R., Kern, S. E., Hruban, R. H., Karchin, R., Papadopoulos, N., Parmigiani, G., Vogelstein, B., Velculescu, V. E.,Kinzler, K. W. (2008): Core signaling pathways in human pancreatic cancers revealed by global genomic analyses. Science 321, 1801-1806.

47. Kanda, M., Matthaei, H., Wu, J., Hong, S. M., Yu, J., Borges, M., Hruban, R. H., Maitra, A., Kinzler, K., Vogelstein, B.,Goggins, M. (2012): Presence of somatic mutations in most early-stage pancreatic intraepithelial neoplasia. Gastroenterology 142, 730-733.e739.

48. Kang, J., Hwang, I., Yoo, C., Kim, K. P., Jeong, J. H., Chang, H. M., Lee, S. S., Park, D. H., Song, T. J., Seo, D. W., Lee, S. K., Kim, M. H., Hong, S. M., Shin, S. H., Hwang, D. W., Song, K. B., Lee, J. H., Kim, S. C.,Ryoo, B. Y. (2018): Nab-paclitaxel plus gemcitabine versus FOLFIRINOX as the first-line chemotherapy for patients with metastatic pancreatic cancer: retrospective analysis. Invest New Drugs 36, 732-741.

49. Kaplan, E. L.,Meier, P. (1958): Nonparametric Estimation from Incomplete Observations. Journal of the American Statistical Association 53, 457-481.

50. Kim, J. E., Lee, K. T., Lee, J. K., Paik, S. W., Rhee, J. C.,Choi, K. W. (2004): Clinical usefulness of carbohydrate antigen 19-9 as a screening test for pancreatic cancer in an asymptomatic population. J Gastroenterol Hepatol 19, 182-186.

51. Kim, M. K., Woo, S. M., Park, B., Yoon, K. A., Kim, Y. H., Joo, J., Lee, W. J., Han, S. S., Park, S. J.,Kong, S. Y. (2018): Prognostic Implications of Multiplex Detection of KRAS Mutations in Cell-Free DNA from Patients with Pancreatic Ductal Adenocarcinoma. Clin Chem 64, 726-734.

52. Kim, S., Signorovitch, J. E., Yang, H., Patterson-Lomba, O., Xiang, C. Q., Ung, B., Parisi, M.,Marshall, J. L. (2018): Comparative Effectiveness of nab-Paclitaxel Plus Gemcitabine vs FOLFIRINOX in Metastatic Pancreatic Cancer: A Retrospective Nationwide Chart Review in the United States. Advances in therapy 35, 1564-1577.

53. Kunzmann, V., Siveke, J. T., Algül, H., Goekkurt, E., Siegler, G., Martens, U., Waldschmidt, D., Pelzer, U., Fuchs, M., Kullmann, F., Boeck, S., Ettrich, T. J., Held, S., Keller, R., Klein, I., Germer, C.-T., Stein, H., Friess, H., Bahra, M., Jakobs, R., Hartlapp, I., Heinemann, V., Hennes, E., Lindig, U., Geer, T., Stahl, M., Senkal, M., Südhoff, T., Egger, M., Kahl, C., Große-Thie, C., Reiser, M., Mahlmann, S., Fix, P., Schulz, H., Maschmeyer, G.,Blau, W. (2021): Nab-paclitaxel plus gemcitabine versus nab-paclitaxel plus gemcitabine followed by FOLFIRINOX induction chemotherapy in locally advanced pancreatic cancer (NEOLAP-AIO-PAK-0113): a multicentre, randomised, phase 2 trial. The Lancet Gastroenterology & Hepatology 6, 128-138.

54. Lambert, A., Schwarz, L., Borbath, I., Henry, A., Van Laethem, J.-L., Malka, D., Ducreux, M.,Conroy, T. (2019): An update on treatment options for pancreatic adenocarcinoma. Therapeutic advances in medical oncology 11, 1758835919875568-1758835919875568.

55. Le, D. T., Durham, J. N., Smith, K. N., Wang, H., Bartlett, B. R., Aulakh, L. K., Lu, S., Kemberling, H., Wilt, C., Luber, B. S., Wong, F., Azad, N. S., Rucki, A. A., Laheru, D., Donehower, R., Zaheer, A., Fisher, G. A., Crocenzi, T. S., Lee, J. J., Greten, T. F., Duffy, A. G., Ciombor, K. K., Eyring, A. D., Lam, B. H., Joe, A., Kang, S. P., Holdhoff, M., Danilova, L., Cope, L., Meyer, C., Zhou, S., Goldberg, R. M., Armstrong, D. K., Bever, K. M., Fader, A. N., Taube, J., Housseau, F., Spetzler, D., Xiao, N., Pardoll, D. M., Papadopoulos, N., Kinzler, K. W., Eshleman, J. R., Vogelstein, B., Anders, R. A.,Diaz, L. A., Jr. (2017): Mismatch repair deficiency predicts response of solid tumors to PD-1 blockade. Science (New York, N.Y.) 357, 409-413.

56. Leon, S. A., Shapiro, B., Sklaroff, D. M.,Yaros, M. J. (1977): Free DNA in the serum of cancer patients and the effect of therapy. Cancer Res 37, 646-650.

57. Ma, J., Siegel, R.,Jemal, A. (2013): Pancreatic Cancer Death Rates by Race Among US Men and Women, 1970–2009. JNCI: Journal of the National Cancer Institute 105, 1694-1700.

58. Mandel, P.,Metais, P. (1948): [Not Available]. C R Seances Soc Biol Fil 142, 241-243.

59. Marabelle, A., Le, D. T., Ascierto, P. A., Giacomo, A. M. D., Jesus-Acosta, A. D., Delord, J.-P., Geva, R., Gottfried, M., Penel, N., Hansen, A. R., Piha-Paul, S. A., Doi, T., Gao, B., Chung, H. C., Lopez-Martin, J., Bang, Y.-J., Frommer, R. S., Shah, M., Ghori, R., Joe, A. K., Pruitt, S. K.,Jr, L. A. D. (2020): Efficacy of Pembrolizumab in Patients With Noncolorectal High Microsatellite Instability/Mismatch Repair–Deficient Cancer: Results From the Phase II KEYNOTE-158 Study. Journal of Clinical Oncology 38, 1-10.

60. Marcus, L., Lemery, S. J., Keegan, P.,Pazdur, R. (2019): FDA Approval Summary: Pembrolizumab for the treatment of microsatellite instability-high solid tumors. Clinical Cancer Research, clincanres.4070.2018.

61. Marrelli, D., Caruso, S., Pedrazzani, C., Neri, A., Fernandes, E., Marini, M., Pinto, E.,Roviello, F. (2009): CA19-9 serum levels in obstructive jaundice: clinical value in benign and malignant conditions. Am J Surg 198, 333-339.

62. Metzenmacher, M., Váraljai, R., Hegedüs, B., Cima, I., Forster, J., Schramm, A., Scheffler, B., Horn, P. A., Klein, C. A., Szarvas, T., Reis, H., Bielefeld, N., Roesch, A., Aigner, C., Kunzmann, V., Wiesweg, M., Siveke, J. T., Schuler, M.,Lueong, S. S. (2020): Plasma Next Generation Sequencing and Droplet Digital-qPCR-Based Quantification of Circulating Cell-Free RNA for Noninvasive Early Detection of Cancer. Cancers (Basel) 12

63. Moffat, G. T.,O'Reilly, E. M. (2020): The role of PARP inhibitors in germline BRCA-associated pancreatic ductal adenocarcinoma. Clin Adv Hematol Oncol 18, 168-179.

64. Mohan, S., Ayub, M., Rothwell, D. G., Gulati, S., Kilerci, B., Hollebecque, A., Sun Leong, H., Smith, N. K., Sahoo, S., Descamps, T., Zhou, C., Hubner, R. A., McNamara, M. G., Lamarca, A., Valle, J. W., Dive, C.,Brady, G. (2019): Analysis of circulating cell-free DNA identifies KRAS copy number gain and mutation as a novel prognostic marker in Pancreatic cancer. Scientific reports 9, 11610-11610.

65. Mouliere, F., Chandrananda, D., Piskorz, A. M., Moore, E. K., Morris, J., Ahlborn, L. B., Mair, R., Goranova, T., Marass, F., Heider, K., Wan, J. C. M., Supernat, A., Hudecova, I., Gounaris, I., Ros, S., Jimenez-Linan, M., Garcia-Corbacho, J., Patel, K., Østrup, O., Murphy, S., Eldridge, M. D., Gale, D., Stewart, G. D., Burge, J., Cooper, W. N., van der Heijden, M. S., Massie, C. E., Watts, C., Corrie, P., Pacey, S., Brindle, K. M., Baird, R. D., Mau-Sørensen, M., Parkinson, C. A., Smith, C. G., Brenton, J. D.,Rosenfeld, N. (2018): Enhanced detection of circulating tumor DNA by fragment size analysis. Sci Transl Med 10

66. Mouliere, F., Robert, B., Arnau Peyrotte, E., Del Rio, M., Ychou, M., Molina, F., Gongora, C.,Thierry, A. R. (2011): High fragmentation characterizes tumour-derived circulating DNA. PLoS One 6, e23418.

67. Mukaka, M. M. (2012): Statistics corner: A guide to appropriate use of correlation coefficient in medical research. Malawi medical journal : the journal of Medical Association of Malawi 24, 69-71.

68. Oettle, H.,Lehmann, T. (2016): Gemcitabine-resistant pancreatic cancer: a second-line option. Lancet 387, 507-508.

69. Pérez-Barrios, C., Nieto-Alcolado, I., Torrente, M., Jiménez-Sánchez, C., Calvo, V., Gutierrez-Sanz, L., Palka, M., Donoso-Navarro, E., Provencio, M.,Romero, A. (2016): Comparison of methods for circulating cell-free DNA isolation using blood from cancer patients: impact on biomarker testing. Translational lung cancer research 5, 665-672.

70. Pietrasz, D., Pécuchet, N., Garlan, F., Didelot, A., Dubreuil, O., Doat, S., Imbert-Bismut, F., Karoui, M., Vaillant, J.-C., Taly, V., Laurent-Puig, P.,Bachet, J.-B. (2017): Plasma Circulating Tumor DNA in Pancreatic Cancer Patients Is a Prognostic Marker. Clinical Cancer Research 23, 116-123.

71. Pishvaian, M. J., Blais, E. M., Brody, J. R., Lyons, E., DeArbeloa, P., Hendifar, A., Mikhail, S., Chung, V., Sahai, V., Sohal, D. P. S., Bellakbira, S., Thach, D., Rahib, L., Madhavan, S., Matrisian, L. M.,Petricoin, E. F., 3rd. (2020): Overall survival in patients with pancreatic cancer receiving matched therapies following molecular profiling: a retrospective analysis of the Know Your Tumor registry trial. Lancet Oncol 21, 508-518.

72. Poruk, K. E., Gay, D. Z., Brown, K., Mulvihill, J. D., Boucher, K. M., Scaife, C. L., Firpo, M. A.,Mulvihill, S. J. (2013): The clinical utility of CA 19-9 in pancreatic adenocarcinoma: diagnostic and prognostic updates. Current molecular medicine 13, 340-351.

73. Provenzano, P. P., Cuevas, C., Chang, A. E., Goel, V. K., Von Hoff, D. D.,Hingorani, S. R. (2012): Enzymatic targeting of the stroma ablates physical barriers to treatment of pancreatic ductal adenocarcinoma. Cancer cell 21, 418-429.

74. Pusceddu, S., Ghidini, M., Torchio, M., Corti, F., Tomasello, G., Niger, M., Prinzi, N., Nichetti, F., Coinu, A., Di Bartolomeo, M., Cabiddu, M., Passalacqua, R., de Braud, F.,Petrelli, F. (2019): Comparative Effectiveness of Gemcitabine plus Nab-Paclitaxel and FOLFIRINOX in the First-Line Setting of Metastatic Pancreatic Cancer: A Systematic Review and Meta-Analysis. Cancers 11, 484.

75. Quante, A. S., Ming, C., Rottmann, M., Engel, J., Boeck, S., Heinemann, V., Westphalen, C. B.,Strauch, K. (2016): Projections of cancer incidence and cancer-related deaths in Germany by 2020 and 2030. Cancer medicine 5, 2649-2656.

76. RKI. (2016): Bericht zum Krebsgeschehen in Deutschland 2016. Berlin: Zentrum für Krebsregisterdaten im Robert Koch-Institut.

77. Rogers, J. C., Boldt, D., Kornfeld, S., Skinner, S. A.,Valeri, C. R. (1972): Excretion of Deoxyribonucleic Acid by Lymphocytes Stimulated with Phytohemagglutinin or Antigen. Proceedings of the National Academy of Sciences 69, 1685-1689.

78. Russo, M., Siravegna, G., Blaszkowsky, L. S., Corti, G., Crisafulli, G., Ahronian, L. G., Mussolin, B., Kwak, E. L., Buscarino, M., Lazzari, L., Valtorta, E., Truini, M., Jessop, N. A., Robinson, H. E., Hong, T. S., Mino-Kenudson, M., Di Nicolantonio, F., Thabet, A., Sartore-Bianchi, A., Siena, S., Iafrate, A. J., Bardelli, A.,Corcoran, R. B. (2016): Tumor Heterogeneity and Lesion-Specific Response to Targeted Therapy in Colorectal Cancer. Cancer Discovery 6, 147-153.

79. Sausen, M., Phallen, J., Adleff, V., Jones, S., Leary, R. J., Barrett, M. T., Anagnostou, V., Parpart-Li, S., Murphy, D., Kay Li, Q., Hruban, C. A., Scharpf, R., White, J. R., O'Dwyer, P. J., Allen, P. J., Eshleman, J. R., Thompson, C. B., Klimstra, D. S., Linehan, D. C., Maitra, A., Hruban, R. H., Diaz, L. A., Von Hoff, D. D., Johansen, J. S., Drebin, J. A.,Velculescu, V. E. (2015): Clinical implications of genomic alterations in the tumour and circulation of pancreatic cancer patients. Nature Communications 6, 7686.

80. Schwarzenbach, H., Eichelser, C., Kropidlowski, J., Janni, W., Rack, B.,Pantel, K. (2012): Loss of heterozygosity at tumor suppressor genes detectable on fractionated circulating cell-free tumor DNA as indicator of breast cancer progression. Clin Cancer Res 18, 5719-5730.

81. Sorber, L., Zwaenepoel, K., Deschoolmeester, V., Roeyen, G., Lardon, F., Rolfo, C.,Pauwels, P. (2017): A Comparison of Cell-Free DNA Isolation Kits: Isolation and Quantification of Cell-Free DNA in Plasma. J Mol Diagn 19, 162-168.

82. Sorenson, G. D., Pribish, D. M., Valone, F. H., Memoli, V. A., Bzik, D. J.,Yao, S. L. (1994): Soluble normal and mutated DNA sequences from single-copy genes in human blood. Cancer Epidemiology Biomarkers & Prevention 3, 67-71.

83. Sousa, C. M., Biancur, D. E., Wang, X., Halbrook, C. J., Sherman, M. H., Zhang, L., Kremer, D., Hwang, R. F., Witkiewicz, A. K., Ying, H., Asara, J. M., Evans, R. M., Cantley, L. C., Lyssiotis, C. A.,Kimmelman, A. C. (2016): Pancreatic stellate cells support tumour metabolism through autophagic alanine secretion. Nature 536, 479-483.

84. Strijker, M., Soer, E. C., de Pastena, M., Creemers, A., Balduzzi, A., Beagan, J. J., Busch, O. R., van Delden, O. M., Halfwerk, H., van Hooft, J. E., van Lienden, K. P., Marchegiani, G., Meijer, S. L., van Noesel, C. J., Reinten, R. J., Roos, E., Schokker, S., Verheij, J., van de Vijver, M. J., Waasdorp, C., Wilmink, J. W., Ylstra, B., Besselink, M. G., Bijlsma, M. F., Dijk, F.,van Laarhoven, H. W. (2020): Circulating tumor DNA quantity is related to tumor volume and both predict survival in metastatic pancreatic ductal adenocarcinoma. International journal of cancer 146, 1445-1456.

85. Sugimori, M., Sugimori, K., Tsuchiya, H., Suzuki, Y., Tsuyuki, S., Kaneta, Y., Hirotani, A., Sanga, K., Tozuka, Y., Komiyama, S., Sato, T., Tezuka, S., Goda, Y., Irie, K., Miwa, H., Miura, Y., Ishii, T., Kaneko, T., Nagahama, M., Shibata, W., Nozaki, A.,Maeda, S. (2020): Quantitative monitoring of circulating tumor DNA in patients with advanced pancreatic cancer undergoing chemotherapy. Cancer science 111, 266-278.

86. Tempero, M. A., Uchida, E., Takasaki, H., Burnett, D. A., Steplewski, Z.,Pour, P. M. (1987): Relationship of carbohydrate antigen 19-9 and Lewis antigens in pancreatic cancer. Cancer Res 47, 5501-5503.

87. Tjensvoll, K., Lapin, M., Buhl, T., Oltedal, S., Steen-Ottosen Berry, K., Gilje, B., Søreide, J. A., Javle, M., Nordgård, O.,Smaaland, R. (2016): Clinical relevance of circulating KRAS mutated DNA in plasma from patients with advanced pancreatic cancer. Molecular oncology 10, 635-643.

88. Toledano-Fonseca, M., Cano, M. T., Inga, E., Rodríguez-Alonso, R., Gómez-España, M. A., Guil-Luna, S., Mena-Osuna, R., de la Haba-Rodríguez, J. R., Rodríguez-Ariza, A.,Aranda, E. (2020): Circulating Cell-Free DNA-Based Liquid Biopsy Markers for the Non-Invasive Prognosis and Monitoring of Metastatic Pancreatic Cancer. Cancers 12, 1754.

89. Treadwell, J. R., Zafar, H. M., Mitchell, M. D., Tipton, K., Teitelbaum, U.,Jue, J. (2016): Imaging Tests for the Diagnosis and Staging of Pancreatic Adenocarcinoma: A Meta-Analysis. Pancreas 45, 789-795.

90. Untawale, S., Zorbas, M., Hodgson, C., Coffey, R., Gallick, G., North, S., Wildrick, D., Olive, M., Blick, M.,Yeoman, L. (1993): Transforming Growth Factor-α Production and Autoinduction in a Colorectal Carcinoma Cell Line (DiFi) with an Amplified Epidermal Growth Factor Receptor Gene. Cancer research 53, 1630-1636.

91. Vincent, A., Herman, J., Schulick, R., Hruban, R. H.,Goggins, M. (2011): Pancreatic cancer. Lancet (London, England) 378, 607-620.

92. Von Hoff, D. D., Ervin, T., Arena, F. P., Chiorean, E. G., Infante, J., Moore, M., Seay, T., Tjulandin, S. A., Ma, W. W., Saleh, M. N., Harris, M., Reni, M., Dowden, S., Laheru, D., Bahary, N., Ramanathan, R. K., Tabernero, J., Hidalgo, M., Goldstein, D., Van Cutsem, E., Wei, X., Iglesias, J.,Renschler, M. F. (2013): Increased Survival in Pancreatic Cancer with nab-Paclitaxel plus Gemcitabine. New England Journal of Medicine 369, 1691-1703.

93. Waddell, N., Pajic, M., Patch, A.-M., Chang, D. K., Kassahn, K. S., Bailey, P., Johns, A. L., Miller, D., Nones, K., Quek, K., Quinn, M. C. J., Robertson, A. J., Fadlullah, M. Z. H., Bruxner, T. J. C., Christ, A. N., Harliwong, I., Idrisoglu, S., Manning, S., Nourse, C., Nourbakhsh, E., Wani, S., Wilson, P. J., Markham, E., Cloonan, N., Anderson, M. J., Fink, J. L., Holmes, O., Kazakoff, S. H., Leonard, C., Newell, F., Poudel, B., Song, S., Taylor, D., Waddell, N., Wood, S., Xu, Q., Wu, J., Pinese, M., Cowley, M. J., Lee, H. C., Jones, M. D., Nagrial, A. M., Humphris, J., Chantrill, L. A., Chin, V., Steinmann, A. M., Mawson, A., Humphrey, E. S., Colvin, E. K., Chou, A., Scarlett, C. J., Pinho, A. V., Giry-Laterriere, M., Rooman, I., Samra, J. S., Kench, J. G., Pettitt, J. A., Merrett, N. D., Toon, C., Epari, K., Nguyen, N. Q., Barbour, A., Zeps, N., Jamieson, N. B., Graham, J. S., Niclou, S. P., Bjerkvig, R., Grützmann, R., Aust, D., Hruban, R. H., Maitra, A., Iacobuzio-Donahue, C. A., Wolfgang, C. L., Morgan, R. A., Lawlor, R. T., Corbo, V., Bassi, C., Falconi, M., Zamboni, G., Tortora, G., Tempero, M. A., Australian Pancreatic Cancer Genome, I., Gill, A. J., Eshleman, J. R., Pilarsky, C., Scarpa, A., Musgrove, E. A., Pearson, J. V., Biankin, A. V.,Grimmond, S. M. (2015): Whole genomes redefine the mutational landscape of pancreatic cancer. Nature 518, 495-501.

94. Wang-Gillam, A., Li, C. P., Bodoky, G., Dean, A., Shan, Y. S., Jameson, G., Macarulla, T., Lee, K. H., Cunningham, D., Blanc, J. F., Hubner, R. A., Chiu, C. F., Schwartsmann, G., Siveke, J. T., Braiteh, F., Moyo, V., Belanger, B., Dhindsa, N., Bayever, E., Von Hoff, D. D.,Chen, L. T. (2016): Nanoliposomal irinotecan with fluorouracil and folinic acid in metastatic pancreatic cancer after previous gemcitabine-based therapy (NAPOLI-1): a global, randomised, open-label, phase 3 trial. Lancet 387, 545-557.

95. Watanabe, F., Suzuki, K., Tamaki, S., Abe, I., Endo, Y., Takayama, Y., Ishikawa, H., Kakizawa, N., Saito, M., Futsuhara, K., Noda, H., Konishi, F.,Rikiyama, T. (2019): Longitudinal monitoring of KRAS-mutated circulating tumor DNA enables the prediction of prognosis and therapeutic responses in patients with pancreatic cancer. PloS one 14, e0227366-e0227366.

96. Wolfgang, C. L., Herman, J. M., Laheru, D. A., Klein, A. P., Erdek, M. A., Fishman, E. K.,Hruban, R. H. (2013): Recent progress in pancreatic cancer. CA: a cancer journal for clinicians 63, 318-348.

97. Yadav, D. K., Bai, X., Yadav, R. K., Singh, A., Li, G., Ma, T., Chen, W.,Liang, T. (2018): Liquid biopsy in pancreatic cancer: the beginning of a new era. Oncotarget 9, 26900-26933.

98. Zhan, H. X., Xu, J. W., Wu, D., Wu, Z. Y., Wang, L., Hu, S. Y.,Zhang, G. Y. (2017): Neoadjuvant therapy in pancreatic cancer: a systematic review and meta-analysis of prospective studies. Cancer Med 6, 1201-1219.

99. Zhang, L., Sanagapalli, S.,Stoita, A. (2018): Challenges in diagnosis of pancreatic cancer. World journal of gastroenterology 24, 2047-2060.

100. Zhu, Y., Zhang, H., Chen, N., Hao, J., Jin, H.,Ma, X. (2020): Diagnostic value of various liquid biopsy methods for pancreatic cancer: A systematic review and meta-analysis. Medicine (Baltimore) 99, e18581.

8 TABLES

9 FIGURES

10 ABBREVIATIONS

5-FU	5-fluoruracil	14
AJCC	American joint Committee on Cancer	11
ATM	ataxia-teleangiesctasia mutated	70
BORR	best-overall-response-rate	62
BRAF	protooncogene B-Raf	15
BRCA1	*Breast Cancer Gene 1*	15
BRCA2	*Breast Cancer Gene 2*	15
CA 19-9	carbohydrate antigen 19-9	10
CATO	Computer aided therapy for oncology	22
CDKN2A	cyclin dependent kinase inhibitor 2A	8
cfDNA	cell-free DNA	17
cfRNA	Cell-free RNA	19
CI	Confidence interval	59
CT	computed tomography	10
CTC	circulating tumor cells	17
ctDNA	circulating tumor DNA	17
ddPCR	digital droplet PCR	19
DDR	deoxyribonucleic acid damage repair	15
DNA	deoxyribonucleic acid	15
ECOG	Eastern Cooperative Oncology Group	48
EUS	endoscopic ultrasound	10
FOLFIRINOX	oxaliplatin, irinotecan, leucovorin, fluorouracil	13
FOLFOX	5-FU, folinic acid and oxaliplatin	43
GNAS	guanine nucleotide binding protein	70
HR	Hazard Ratio	59
KRAS	Kirsten Rat Sarcoma	7
LDH	Lactate dehydrogenase	54
MAF	mutational allele fraction	41
MAPK	mitogen-activated protein kinase	15
MRI	magnetic resonance imaging	10
MSI	Microsatellite instability	16
NAPOLI	nanoliposomal irinotecan, 5-fluoruracil (5-FU) and folinic acid	14
NGS	next-generation sequencing	19
OS	Overall Survival	25
PARP	poly-adenosine-diphosphate-ribose polymerase	15
PCR	polymerase chain reaction	19
PD-1	programmed cell death protein 1	16
PDAC	pancreatic ductal adenocarcinoma	7
PFS	progression-free survival	19
RECIST	Response Evaluation Criteria in Solid Tumors	23
SMAD4	mothers against decapentaplegic homolog 4	9
T0	therapy-naive sampling time point	41
TGF-beta	transforming growth factor beta pathway	8
TP53	tumor protein 53	8
TSC1	Tuberous Sclerosis 1	70
TTF	Time-to-treatment failure	25
UICC	Union for international Cancer Control	11
WHO	World Health Organization	22
WTZ	Westdeutsches Tumorzentrum	22

11 ACKNOWLEDGEMENT

At this point I would like to express my gratitude to all the people that have supported me throughout the process of this thesis.

My special thanks goes to my supervisor, Professor Jens Siveke, for your expertise, that has inspired the idea for this thesis. Your excellent mentoring has helped me a lot to keep my focus during this work.

Furthermore, I want to thank my tutors Dr. Smith Sengkwawoh Lueong and Dr. Sven-Thorsten Liffers who thaught me a lot with their constructive feedback. The intensive discussions with you pushed me to sharpen my thinking and helped me to improve my work.

Finally, I want to thank my family, especially my parents Dr. Bettina Rudolph and Dr. Roland Rudolph and my brother Dr. Jens Rudolph, for their emotional support during the process of this work. Your words and advise kept me motivated and I am very grateful to have such wonderful supporters at my side during this journey.

12 CURRICULUM VITAE

The Curriculum Vitae is not included in the online version due to privacy reasons.